

# Diagnostic Uncertainty Calibration: Towards Reliable Machine Predictions in Medical Domain

A PREPRINT

Takahiro Mimori<sup>1</sup>, Keiko Sasada<sup>2</sup>, Hiroataka Matsui<sup>2,3</sup>, Issei Sato<sup>1,4</sup>

<sup>1</sup>RIKEN AIP

<sup>2</sup>Kumamoto University Hospital, Kumamoto University

<sup>3</sup>Faculty of Life Sciences, Kumamoto University

<sup>4</sup>The University of Tokyo

takahiro.mimori@riken.jp, {ksasada@kuh., hmatsui@}kumamoto-u.ac.jp, sato@k.u-tokyo.ac.jp

July 8, 2020

## ABSTRACT

Label disagreement between human experts is a common issue in the medical domain and poses unique challenges in the evaluation and learning of classification models. In this work, we extend metrics for probability prediction, including calibration, *i.e.*, the reliability of predictive probability, to adapt to such a situation. We further formalize the metrics for higher-order statistics, including inter-rater disagreement, in a unified way, which enables us to assess the quality of distributional uncertainty. In addition, we propose a novel post-hoc calibration method that equips trained neural networks with calibrated distributions over class probability estimates. With a large-scale medical imaging application, we show that our approach significantly improves the quality of uncertainty estimates in multiple metrics.

## 1 Introduction

Reliable uncertainty quantification is an indispensable property for safety-critical systems such as medical diagnosis assistance. Despite the high accuracy of modern neural networks in the wide-ranging classification tasks, their predictive probability often tends to be uncalibrated [10]. Measuring and improving probability calibration, which is the closeness of predictive probability to an actual class frequency, has become one of the central issues in machine learning research [34, 36, 19]. At the same time, uncertainty exists in the real-world labels used as ground truth for training classifiers. Notably, in the medical domain, inter-rater variability of annotations is commonly observed despite their expertise [25, 28, 13]. As current machine learning research primarily relies on ground truth labels, evaluation and learning of classifiers under the label uncertainty poses unique challenges in the medical domain.

To obtain reliable class probability estimates (CPEs) from a trained classifier, *post-hoc* calibration, which transforms the classifier’s output scores to fit into empirical class probabilities, has been proposed for both general classifiers [24, 37, 38] and neural networks [10, 18]. However, current evaluation metrics for calibration rely on an empirical accuracy calculated with ground truth, in which the uncertainty of labels has not been considered. Moreover, an essential aspect of uncertainty is not fully accounted for by CPEs, *e.g.*, whether a 50% confidence of class  $x$  comes from machine’s unconfidence or human’s disagreement about classification is not differentiated, even when the CPE matches an observed label frequency in expectation. Recent work [25] has indicated that label-side uncertainty measures, such as an empirical disagreement frequency, inferred from CPEs, is suboptimal. They instead used the direct discrimination of high uncertainty instances with input features as a superior approach. However, this treatment requires training an additional predictor per different objective and lacks an integrated view of the problem with classification. Also, since the discrimination threshold is given in a problem-specific way, how such a prediction should be expressed and evaluated in a general situation has not been formalized.

In this work, we first develop an evaluation framework for CPEs under label uncertainty, in which multiple annotations per instance (called *label histograms*) is available. With the insight gained from proper scoring rules [9] and their decomposition [5], we extend existing metrics, including calibration measures, for the situation with label histograms. Next, we generalize our formulation for probabilistic predictions on higher-order statistics, including inter-rater disagreement, which enables us to evaluate these statistics in a unified way with CPEs. At the same time, the importance of awareness for the distribution of CPEs is emphasized for the reliable predictions on the statistics. To fit into this situation, we propose a novel approach that enhances the reliability of neural network models in terms of CPE distributions. While our approach, which we referred to  $\alpha$ -calibration, only uses a single parameter to control the distribution, it can enable us to capture well-recognized notions of uncertainty: epistemic and aleatoric [6, 29, 15] within the distributional model. Finally, we apply our evaluation frameworks and the  $\alpha$ -calibration to a large-scale classification task of cellular image data provided from a study of myelodysplastic syndrome (MDS) [28]. We show that our uncertainty-aware evaluation metrics for CPEs offer a meaningful interpretation of classification performance. Also, the  $\alpha$ -calibration shows a significant improvement in the prediction of disagreement between annotators.

## 2 Background

We overview calibration measures and proper scoring rules as a prerequisite for our work.

### 2.1 Notation

Let  $K \in \mathbb{N}$  be a number of categories,  $e^K = \{e_1, \dots, e_K\}$  be a set of  $K$  dimensional one-hot vectors (i.e.,  $e_{kl} = \delta_{kl}$ ), and  $\Delta^{K-1} := \{\zeta \in \mathbb{R}_{\geq 0}^K : \sum_k \zeta_k = 1\}$  be a  $K - 1$ -dimensional probability simplex. Let  $(X, Y)$  be jointly distributed random variables over  $\mathcal{X}$  and  $e^K$ , where  $X$  denotes an input feature, such as an image data, and  $Y$  denotes a  $K$ -way label. Given a classification model  $f : \mathcal{X} \rightarrow e^K$ , a predictive class probability of the model for an input feature  $X$  is also a random variable and denoted by  $Z = (Z_1, \dots, Z_K)^\top = f(X) \in \Delta^{K-1}$ .

### 2.2 Calibration measures

The notion of calibration, which is an agreement between a predictive class probability and an empirical class frequency, is a desirable property for the prediction to be reliable. Formally, we reference [17] for the definition of calibration.

**Definition 1** (Calibration).<sup>1</sup> A classification model  $f : \mathcal{X} \rightarrow e^K$  is said to be *calibrated* if its predictive probability  $Z = f(X) \in \Delta^{K-1}$  satisfies  $\forall k, Z_k = C_k := P(Y = e_k | Z)$ , where  $C := (C_1, \dots, C_K)^\top \in \Delta^{K-1}$  is called a calibration map.

The following metric is commonly used to measure an error of calibration for binary classifiers:

**Definition 2** (Calibration Error for Binary Classifier).

$$\text{CE}_1 := (\mathbb{E}[|Z_1 - C_1|^p])^{1/p}, \quad \text{where } p \geq 1. \quad (1)$$

Note that a case of  $p = 2$  is called a squared calibration error [19] and  $p = 1$  is an expectation calibration error (ECE) [23]. CE takes a minimum value 0 iff  $Z = C$ . We refer to CE as a case of  $p = 2$  in this work. For multiclass cases, we use a commonly used definition of class-wise calibration error [19], which is defined as  $\text{CE} := (\sum_k \text{CE}_k^2)^{1/2}$ .

### 2.3 Proper scoring rules

Although calibration is a desirable property, being calibrated is not sufficient for useful predictions. For instance, a predictor that always presents the marginal class frequency  $Z = (P(Y = e_1), \dots, P(Y = e_K))^\top$  is perfectly calibrated, but entirely lacks the sharpness of prediction for labels stratified with  $Z$ . In contrast, the strictly proper scoring rules [9] elicit an instance-wise true probability in expectation and do not suffer from this problem.

**Definition 3** (Proper scoring rules for classification). A loss function  $\ell : e^K \times \Delta^{K-1} \rightarrow \mathbb{R}$  is said to be *proper* if  $\forall q \in \Delta^{K-1}, \forall z \in \Delta^{K-1}$  s.t.  $z \neq q$ ,

$$\mathbb{E}_{Y \sim \text{Cat}(q)}[\ell(Y, z)] \geq \mathbb{E}_{Y \sim \text{Cat}(q)}[\ell(Y, q)] \quad (2)$$

holds, where  $\text{Cat}(\cdot)$  denotes a categorical distribution. If the strict inequality holds,  $\ell$  is said to be *strictly proper*. Following the convention, we write  $\ell(q, z) = \mathbb{E}_{Y \sim \text{Cat}(q)}[\ell(Y, z)]$  for  $q \in \Delta^{K-1}$ .

<sup>1</sup>Stronger notion of the calibration that requires  $Z = C$  is also used in the literature [34, 36].

For a strictly proper loss  $\ell$ , the divergence function  $d(q, z) := \ell(q, z) - \ell(q, q)$  takes a non-negative value and is zero iff  $z = q$ , by definition. Squared loss  $\ell_{\text{sq}}(y, z) := \|y - z\|^2$  and logarithmic loss  $\ell_{\log}(y, z) := -\sum_k y_k \log z_k$  are the most well known examples of strictly proper losses. For these cases, the divergence functions are given as  $d_{\text{sq}}(q, z) = \ell_{\text{sq}}(q, z)$  and  $d_{\log}(q, z) = D_{\text{KL}}(q, z)$ , a.k.a. KL divergence, respectively.

Let  $L := \mathbb{E}[d(Y, Z)] = \mathbb{E}[d(Y, f(X))]$  denote the expected loss, where the expectation is taken over a distribution  $P(X, Y)$ . As special examples of  $L$  that base on the  $\frac{1}{2}\ell_{\text{sq}}$  and  $\ell_{\text{sq}}$ ,

$$L_{\text{sq}'} := \mathbb{E} \left[ \frac{1}{2} \ell_{\text{sq}}(Y, Z) \right] = \mathbb{E}[(Y_1 - Z_1)^2] \quad \text{for } K = 2, \quad (3)$$

$$L_{\text{sq}} := \mathbb{E}[\ell_{\text{sq}}(Y, Z)] = \mathbb{E}[\|Y - Z\|^2] \quad \text{for } K \geq 2, \quad (4)$$

are commonly used for binary and multiclass case, respectively. When the expectation is taken over an empirical distribution  $P_{\text{emp}}(X, Y)$ , these are equivalent to Brier score (BS) and probability score (PS), respectively [2, 22].

## 2.4 Decomposition of proper losses

The relation between the expected proper loss  $L$  and the calibration measures is clarified with a decomposition of  $L$  as follows [5]:

$$L = \text{CL} + \text{RL}, \quad \text{where} \quad \begin{cases} \text{CL} := \mathbb{E}[d(C, Z)], & \text{(Calibration Loss)} \\ \text{RL} := \mathbb{E}[d(Y, C)]. & \text{(Refinement Loss)} \end{cases} \quad (5)$$

The CL term corresponds to an error of calibration because the term will be zero iff  $Z$  equals the calibration map  $C = \mathbb{E}[Y|Z]$ . Complementary, the RL term, which represents the divergence of  $Y$  from  $\mathbb{E}[Y|Z]$ , shows the dispersion of labels  $Y$  given  $Z$  from its mean  $\mathbb{E}[Y|Z]$  averaged over  $Z$ . The relation between CL and calibration errors:  $\text{CL}_{\text{sq}'} = \text{CE}^2$ ,  $\text{CL}_{\text{sq}} = \text{CE}^2$  are also confirmed for binary and multiclass cases, respectively.

Under an assumption that labels follow an instance-wise categorical distribution as  $Y|X \sim \text{Cat}(Q)$ , where  $Q(X) \in \Delta^{K-1}$ , Kull and Flach [17] further decompose  $L$  into the following terms:<sup>2</sup>

$$L = \underbrace{\text{CL} + \text{ERL}}_{\text{EL}} + \text{IL}, \quad \text{where} \quad \begin{cases} \text{EL} = \mathbb{E}[d(Q, Z)], & \text{(Epistemic Loss)} \\ \text{IL} = \mathbb{E}[d(Y, Q)], & \text{(Irreducible Loss)} \\ \text{ERL} = \mathbb{E}[d(Q, C)]. & \text{(Epistemic Refinement Loss)} \end{cases} \quad (6)$$

The EL term is the loss due to the non-optimality of the model. The IL term stemming from the randomness of observations is called *aleatoric uncertainty* in the literature [6, 29]. We refer to Appendix A for details and proofs of the statements in this section.

## 3 Evaluation of class probability estimates with label histograms

Now, we formalize the evaluation metrics of class probability estimates (CPEs) for label histograms, where multiple labels per instance are observed. We assume that  $N$  input samples are obtained in an i.i.d. manner:  $\{x_i\}_{i=1}^N \sim P(X)$ , and for each instance  $i$ , label histogram  $y_i \in \mathbb{Z}_{\geq 0}^K$  is obtained from  $n_i$  annotators in a conditionally i.i.d. manner, i.e.,  $\{y_i^{(j)} \in e^K\}_{j=1}^{n_i} | x_i \sim P(Y|X = x_i)$  and  $y_i = \sum_{j=1}^{n_i} y_i^{(j)}$ . A predictive class probability for the  $i$ -th instance is denoted by  $z_i = f(x_i) \in \Delta^{K-1}$ . While the terms such as EL and CL in the previous section depends on the choice of  $\ell$  and  $L$ , we assume  $\ell_{\text{sq}}$  and  $L_{\text{sq}}$  in equation (4) for those and omit indexes from the other terms for notational simplicity.

### 3.1 Estimators of expected squared and epistemic loss

We first derive an unbiased estimator of the expected squared loss  $L_{\text{sq}}$  from label histograms.

**Proposition 1** (Unbiased estimator of expected squared loss). The following estimator of  $L_{\text{sq}}$  is unbiased.

$$\hat{L}_{\text{sq}} := \frac{1}{W} \sum_{i=1}^N w_i \sum_{k=1}^K [(\hat{\mu}_{ik} - z_{ik})^2 + \hat{\mu}_{ik}(1 - \hat{\mu}_{ik})], \quad (7)$$

where  $\hat{\mu}_{ik} := y_{ik}/n_i$ ,  $w_i \geq 0$ , and  $W := \sum_{i=1}^N w_i$ .

<sup>2</sup>The original paper refers to the ERL term as grouping loss (GL).

Note that an optimal weight vector  $w$  that minimizes a variance  $\mathbb{V}[\widehat{L}_{\text{sq}}]$  would be  $w = 1$  if the number of annotators  $n_i$  is a constant for all the instances. Otherwise, it depends on undetermined terms, as discussed in Appendix B. We use  $w = 1$  as a standard choice, where  $\widehat{L}_{\text{sq}}$  coincides with the probability score PS when every instance has a single label.

In addition to letting  $\widehat{L}_{\text{sq}}$  have higher statistical power than single-labeled cases, label histograms also enable us to directly estimate the epistemic loss EL, which is a discrepancy measure from the optimal model. A plugin estimator of EL is obtained by

$$\widetilde{\text{EL}} := \frac{1}{N} \sum_i \sum_k (\widehat{\mu}_{ik} - z_{ik})^2. \quad (8)$$

However,  $\widetilde{\text{EL}}$  turns out to be severely biased. We can alternatively use an unbiased estimator of EL:

**Proposition 2** (Unbiased estimator of EL). The following estimator of EL is unbiased.

$$\widehat{\text{EL}} := \widetilde{\text{EL}} - \frac{1}{N} \sum_i \sum_k \frac{1}{n_i - 1} \widehat{\mu}_{ik} (1 - \widehat{\mu}_{ik}). \quad (9)$$

The second correction term implies that  $\widehat{\text{EL}}$  can only be evaluated when more than one label per instance is available. The bias correction effect is significant for a small  $n_i$ , which is relevant to most of the medical applications.

### 3.2 Calibration loss

Relying on the connection between CL and CE, we focus on evaluating CL to measure calibration. The calibration loss is further decomposed into class-wise terms as follows:

$$\text{CL} = \sum_k \text{CL}_k, \quad \text{CL}_k := \mathbb{E}[(C_k - Z_k)^2] = \mathbb{E}[\mathbb{E}[(C_k - Z_k)^2 | Z_k]]. \quad (10)$$

Thus, a case of  $\text{CL}_k$  is sufficient for subsequent discussion. Note that a difficulty exists in the estimation of the conditional expectation on  $Z_k$ . We take a standard binning-based approach [37] to evaluate  $\text{CL}_k$  by stratifying with  $Z_k$  values. Specifically,  $Z_k$  is partitioned into  $B_k$  disjoint regions  $\mathcal{B}_k = \{[\zeta_0 = 0, \zeta_1), [\zeta_1, \zeta_2), \dots, [\zeta_{B_k-1}, \zeta_{B_k} = 1]\}$ , and  $\text{CL}_k$  is approximated as follows:

$$\text{CL}_k(\mathcal{B}_k) := \sum_{b=1}^{B_k} \text{CL}_{kb}(\mathcal{B}_k), \quad \text{where} \quad \begin{cases} \text{CL}_{kb}(\mathcal{B}_k) := \mathbb{E}[\mathbb{E}[(\bar{C}_{kb} - \bar{Z}_{kb})^2 | Z_k \in \mathcal{B}_{kb}]], \\ \bar{C}_{kb} := \mathbb{E}[Y_k | Z_k \in \mathcal{B}_{kb}], \\ \bar{Z}_{kb} := \mathbb{E}[Z_k | Z_k \in \mathcal{B}_{kb}], \end{cases} \quad (11)$$

in which  $\text{CL}_k$  is further decomposed into the bin-wise components. A plugin estimator of  $\text{CL}_{kb}$  is derived as follows:

$$\widetilde{\text{CL}}_{kb}(\mathcal{B}_k) := \frac{|I_{kb}|}{N} (\bar{c}_{kb} - \bar{z}_{kb})^2, \quad \text{where} \quad I_{kb} = \{i : z_{ik} \in \mathcal{B}_{kb}\}, \quad \bar{c}_{kb} := \frac{\sum_{i \in I_{kb}} \widehat{\mu}_{ik}}{|I_{kb}|}, \quad \bar{z}_{kb} := \frac{\sum_{i \in I_{kb}} z_{ik}}{|I_{kb}|}. \quad (12)$$

Note that  $|I_{kb}|$  denotes the size of  $I_{kb}$ . We can again improve the estimator by debiasing as follows:

**Proposition 3** (Debiased estimator of  $\text{CL}_{kb}$ ). The plugin estimator of  $\text{CL}_{kb}$  is debiased with the following estimator:

$$\widehat{\text{CL}}_{kb}(\mathcal{B}_k) := \widetilde{\text{CL}}_{kb}(\mathcal{B}_k) - \frac{|I_{kb}|}{N} \frac{\bar{\sigma}_{kb}^2}{|I_{kb}| - 1}, \quad \text{where} \quad \bar{\sigma}_{kb}^2 := \frac{1}{|I_{kb}|} \sum_{i \in I_{kb}} \widehat{\mu}_{ik}^2 - \left( \frac{1}{|I_{kb}|} \sum_{i \in I_{kb}} \widehat{\mu}_{ik} \right)^2. \quad (13)$$

The correction term would inflate for a small-sized bin with high variance term  $\bar{\sigma}_{kb}^2$ . Note that this estimator is also available for single-labeled data, where  $\widehat{\mu}_{ik} = y_{ik}$ . In such a case, the estimator precisely coincides with a debiased estimator of the *reliability* term formerly proposed in meteorological literature [3, 7].

### 3.3 The remainder: dispersion loss

Now, we consider the remainder of the EL term. As we present in equation (6), EL is decomposed into  $\text{CL} + \text{ERL}$ , in which ERL is a loss relating to the lack of predictive sharpness. However, the approximate calibration loss  $\text{CL}(\mathcal{B})$  is known to be underestimated [34, 19] in relation to the coarseness of the selected binning scheme  $\mathcal{B}$ . This tendency is not necessarily harmful because the required resolution of calibration may also depend on application demand. On the other hand, EL does not suffer from a resolution of  $\mathcal{B}$ . We use the difference  $\text{DL} := \text{EL} - \text{CL}(\mathcal{B})$ , which we call dispersion loss, as a complementary term to CL rather than estimating ERL. For single-labeled cases, a similar argument that considers remaining terms arisen from a discretization of predictions is found in [32].

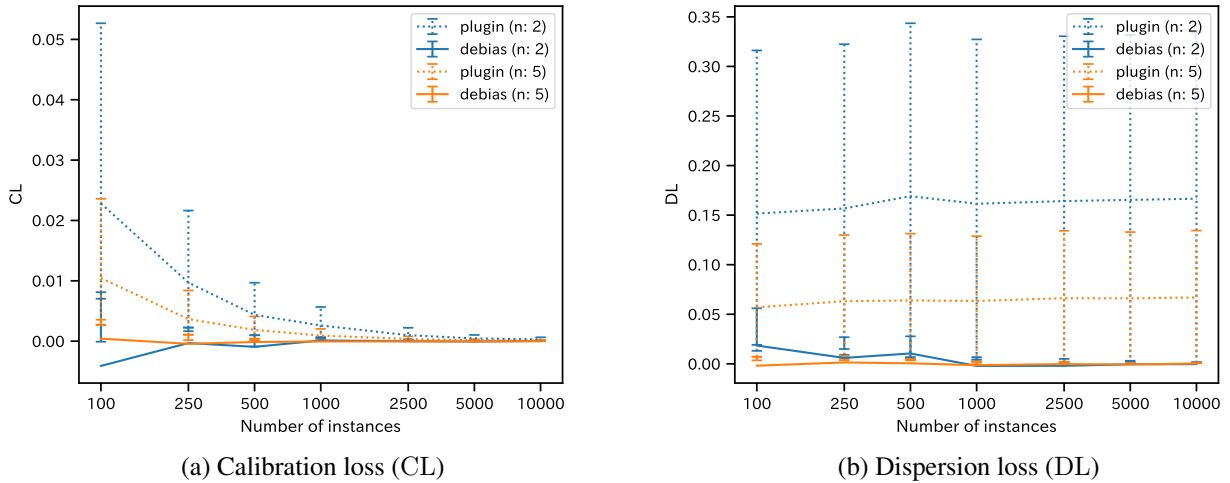


Figure 1: Comparison of the plugin and debiased estimators on synthetic data. For both (a) CL and (b) DL, the debiased estimates are closer to ground truth, which corresponds to 0, than the plugin estimates (dotted lines). The error bars show 90% confidence intervals for the means of 10 runs.

**Proposition 4** (Non-negativity of dispersion loss). Given a binning scheme  $\mathcal{B}$ , a dispersion loss for class  $k$  is decomposed into bin-wise components, where each term takes a non-negative value:

$$DL_k(\mathcal{B}) := EL_k - CL_k(\mathcal{B}) = \sum_b DL_{kb}(\mathcal{B}), \quad (14)$$

$$DL_{kb}(\mathcal{B}) := \mathbb{E}[\mathbb{E}[\{(Q_k - \bar{C}_{kb}) - (Z_k - \bar{Z}_{kb})\}^2 | Z_k \in \mathcal{B}_{kb}]] \geq 0. \quad (15)$$

The proof is shown in Appendix B. The DL term represents an average of the bin-wise overdispersion of the true class probability  $Q_k$ , which is unaccounted for by the deviation of  $Z_k$ . The plugin and debiased estimators of DL are derived from those of EL and CL. In parallel to the relation  $CL = CE^2$ , we call  $DE := DL^{1/2}$  as a dispersion error.

### 3.4 Debiasing effects of CL and DL estimators

To confirm the effect of debiased estimators of CL and DL compared with the plugin estimators, we run experiments in the case of the ideal binary predictor with varying sizes of instances. As shown in Fig. 1, the debiased estimators significantly reduce the plugin estimators' biases, even in the cases with two annotators. Details of the experimental setup are described in Appendix B.

## 4 Evaluation of higher-order statistics

Here, we generalize our framework to evaluate predictions on higher-order statistics. As is done for CPEs, the expected proper losses and calibration measures can also be formalized. We focus on a family of symmetric binary statistics  $\phi : e^{K \times n} \rightarrow \{0, 1\}$  calculated from  $n$  distinct  $K$ -way labels for the same instance. In particular, we evaluate the following statistics in our experiments:

- $\phi^D := \mathbb{I}[Y^{(1)} \neq Y^{(2)}]$ : disagreement between paired labels  $(Y^{(1)}, Y^{(2)})$
- $\phi^{D_k} := \mathbb{I}[Y_k^{(1)} \neq Y_k^{(2)}]$ : disagreement between paired labels  $(Y^{(1)}, Y^{(2)})$  about a specific class  $k$

where an estimator of  $\mathbb{E}[\phi^D | X]$  is known as the Gini-Simpson index used for a measure of diversity.

Given a function  $\varphi : \mathcal{X} \rightarrow [0, 1]$  that represents a predictive probability of being  $\phi = 1$ , a closeness of  $\varphi(X)$  to a true probability  $P(\phi = 1 | X)$  is consistently evaluated with the expected (one dimensional) squared loss  $L_\phi := \mathbb{E}[(\phi - \varphi)^2]$ .

Then, the calibration loss  $CL_\phi$  is derived by applying equation (5) as follows:

$$L_\phi = \underbrace{\mathbb{E}[(\mathbb{E}[\phi|\varphi] - \varphi)^2]}_{CL_\phi} + \underbrace{\mathbb{E}[(\phi - \mathbb{E}[\phi|\varphi])^2]}_{RL_\phi}. \quad (16)$$

An unbiased estimator of  $L_\phi$  and a debiased estimator of  $CL_\phi$  can be derived following a similar discussion as in CPEs. The most different point from the case of CPEs is that it requires more careful consideration to obtain an unbiased estimator of  $\mu_{\phi,i} := \mathbb{E}[\phi|X = x_i]$  as follows:

$$\hat{\mu}_{\phi,i} := \binom{n_i}{n}^{-1} \sum_{j \in \text{Comb}(n_i, n)} \phi(y_i^{(j_1)}, \dots, y_i^{(j_n)}), \quad (17)$$

where  $\text{Comb}(n_i, n)$  denotes the distinct subset of size  $n$  drawn from  $\{1, \dots, n_i\}$  without replacement. The proof is directly followed from the fact that  $\hat{\mu}_{\phi,i}$  is a U-statistic of  $n$ -sample symmetric kernel function  $\phi$  [12]. Details of the derivations for  $\hat{L}_\phi$  and  $\widehat{CL}_\phi$  are described in Appendix C.

Table 1: Summary of evaluation metrics introduced for label histograms

Order	Signature	Description	Rater
1	$L_{\text{sq}} = \text{EL} + \text{IL}$	Expected squared loss of CPEs	$\geq 1$
	$\text{EL} = \text{CL} + \text{DL}$	Epistemic loss of CPEs	$\geq 2$
	$\text{CL} = \text{CE}^2$	Calibration loss of CPEs	$\geq 1$
	$\text{DL} = \text{DE}^2$	Dispersion loss of CPEs	$\geq 2$
2	$L_\phi, \text{CL}_\phi(\phi = \phi^{\text{D}})$	Expected and calibration loss of disagreement	$\geq 2$
	$L_\phi, \text{CL}_\phi(\phi = \phi^{\text{D}\kappa})$	Expected and calibration loss of class-wise disagreement	$\geq 2$

## 5 Post-hoc uncertainty calibration for deep neural networks

Here, we discuss how neural network models can be improved in terms of uncertainty estimation after training. We briefly overview post-hoc calibration methods for CPEs and highlight the need for CPE distribution for higher-order statistics. Then we introduce a newly devised  $\alpha$ -calibration for distributional calibration of CPEs.

### 5.1 Calibration of CPEs for neural networks

The post-hoc calibration of CPEs is commonly performed with a linear transformation of the last layer’s logit vector before softmax activation. In this direction, Guo et al. [10] have extended Platt scaling [24] to propose temperature, vector, and matrix scaling for multiclass problems. Despite its simplicity, the temperature scaling was the most successful one to improve the maximum confident classes’ calibration. Subsequently, Kull et al. [18] have presented an improvement in class-wise calibration errors with vector and matrix scaling. As these approaches maximize a log-likelihood of validation data, we can apply them to the label histograms similarly as for single-labeled cases. Whereas an exhaustive comparison of CPE calibration methods is out of scope, more recent research [39, 26] have designed nonlinear calibration maps with multiple favorable properties, such as expressiveness, data-efficiency, and accuracy-preservation, simultaneously.

### 5.2 Use of CPE distribution for higher-order statistics

Although we assume that labels for each instance follow an i.i.d. distribution, point estimation of class probability is insufficient to predict the higher-order statistics reliably. For instance, when a CPE of the binary class scored 0.5, a predictive disagreement probability between two independent annotators would be 0.5. However, if each instance’s labels are unanimous for all the observed instances, a more sensible prediction of the disagreement probability would be close to 0 from empirical observation. Generally, we assume that a tendency of disagreement varies with an instance.

In the first place, a relevant CPE distribution seems to be obtained with Bayesian approaches. Among the post-hoc approaches, which are usable after a regular neural networks training, Monte-Carlo dropout (MCDO) [8] and Monte-Carlo batch normalization (MCBN) [33] are two established ones for the purpose. Recently, test-time augmentation (TTA) [1, 35] is also proposed for uncertainty estimation. Despite their simplicity in usage, these methods require predictions multiple times and computationally intensive proportional to the sampling size. An alternative approach is

directly modeling CPE distribution with parametric families. In this direction, the Dirichlet distribution is commonly used for its tractability, as seen in several recent approaches [30, 21, 27, 14] in various applications, such as detection of out of distribution instances and generalization improvement. However, current approaches need customized training processes from scratch and are not designed to apply for training neural networks in a post-hoc manner.

### 5.3 $\alpha$ -calibration: a simple post-hoc distribution calibration method

Here, we propose a novel post-hoc calibration method called  $\alpha$ -calibration to enhance the distributional reliability of CPEs for trained neural networks. The requirement for  $\alpha$ -calibration is neural networks that output CPEs  $z \in \Delta^{K-1}$  and label histograms  $y$ . Specifically,  $\alpha$ -calibration models a CPE distribution with a Dirichlet distribution  $\text{Dir}(z|\alpha)$  and optimize a single parameter  $\alpha_0 = \sum_k \alpha_k$  to capture instance-wise uncertainty. Details of the method are found in Appendix D.2. Despite its simplicity,  $\alpha$ -calibration is flexible enough to capture both extremes of epistemic or aleatoric uncertainty. This property is demonstrated with synthetic experiments in Appendix E. Also,  $\alpha$ -calibration is orthogonally applicable with existing CPE calibration methods. It does not degrade calibrated CPEs by design, as similar to temperature scaling that keeps accuracy.

## 6 Experiments

We evaluated the performance of deep neural networks applied for a large-scale medical imaging dataset of myelodysplastic syndrome (MDS) [28], which contains over 90 thousand hematopoietic cell images obtained from blood specimens from 499 patients with MDS. This study was carried out in collaboration with medical technologists who mainly belong to the Kyushu regional department of the Japanese Society for Laboratory Hematology. The use of peripheral blood smear samples for this study was approved by the ethics committee at Kumamoto University, and the study was performed in accordance with the Declaration of Helsinki. For each of the cellular images, the mean of 5.67 medical technologists annotated the cellular category from 22 subtypes. Accurate classification of the images according to the current standard criterion was difficult for even technologists with expertise. Considering a constraint of high labeling cost with experts in the medical domain, the experiments were conducted with only single labels for a training set, and multiple labels were only used in validation and test set. Details of the experimental setup and parameters used are described in Appendix F.

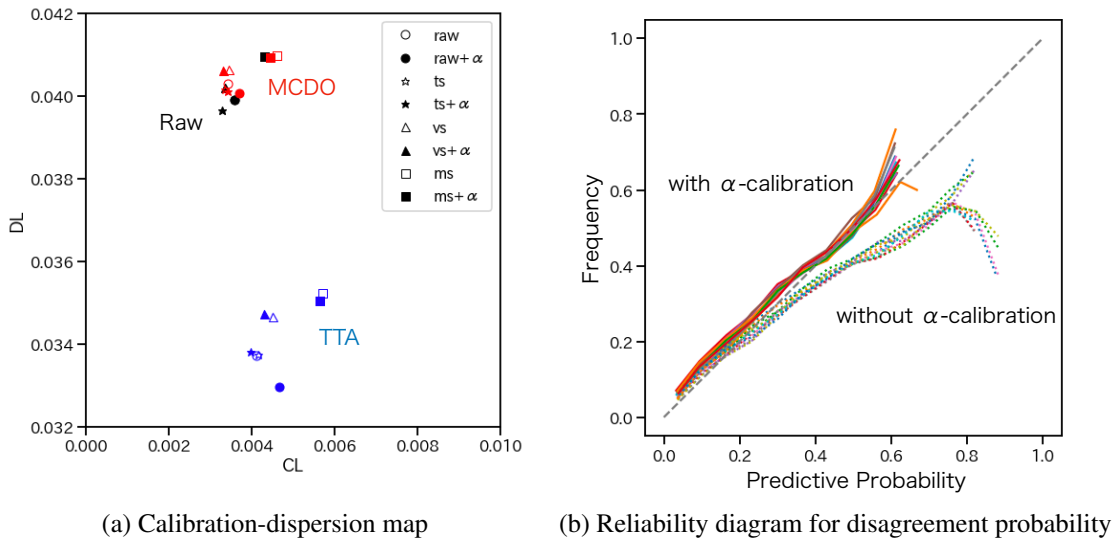


Figure 2: (a) A Calibration-dispersion map for the experiments with MDS data. While TTA predictions deteriorate (increase) the calibration loss ( $\widehat{CL}$ ), they substantially improve (decrease) the dispersion loss ( $\widehat{DL}$ ). (b) A reliability diagram for the inter-rater disagreement probability, where all the methods listed in table 2 are compared. The methods with  $\alpha$ -calibration (solid line) are significantly improved over those without it (dotted line) and aligned to the diagonal line, which corresponds to calibrated predictions.

Table 2: Performance evaluations for MDS data.

Methods		Order 1 metrics			Order 2 metrics	
Pred.	Calib.	Acc $\uparrow$	$\widehat{L}_{sq} \downarrow$	$\widehat{EL} (\widehat{CE}, \widehat{DE}) \downarrow$	$\widehat{L}_{\phi^D} (\widehat{CE}_{\phi^D}) \downarrow$	$\widehat{L}_{\phi^{D*}} (\widehat{CE}_{\phi^{D*}}) \downarrow$
Raw	raw	0.9006	0.2515	0.0435 (0.0600, 0.1998)	0.1477 (0.0628)	0.0153 (0.0168)
	raw + $\alpha$	0.9006	0.2515	0.0435 (0.0600, 0.1998)	<b>0.1454 (0.0406)</b>	<b>0.0151 (0.0098)</b>
	ts	0.9006	<b>0.2509</b>	<b>0.0430 (0.0575, 0.1992)</b>	0.1482 (0.0663)	0.0153 (0.0176)
	ts + $\alpha$	0.9006	<b>0.2509</b>	<b>0.0430 (0.0575, 0.1992)</b>	<b>0.1445 (0.0261)</b>	<b>0.0151 (0.0085)</b>
	vs	<b>0.9010</b>	0.2515	0.0435 (0.0579, 0.2005)	0.1489 (0.0696)	0.0154 (0.0177)
	vs + $\alpha$	<b>0.9010</b>	0.2515	0.0435 (0.0579, 0.2005)	<b>0.1449 (0.0318)</b>	<b>0.0151 (0.0086)</b>
MCDO	raw	0.8983	0.2517	0.0437 (0.0586, 0.2008)	0.1470 (0.0562)	0.0152 (0.0141)
	raw + $\alpha$	0.8996	0.2518	0.0438 (0.0610, <b>0.2002</b> )	<b>0.1450 (0.0346)</b>	<b>0.0151 (0.0091)</b>
	ts	0.8986	<b>0.2515</b>	<b>0.0435 (0.0579, 0.2004)</b>	0.1479 (0.0635)	0.0153 (0.0154)
	ts + $\alpha$	0.8991	<b>0.2515</b>	<b>0.0435 (0.0586, 0.2003)</b>	<b>0.1442 (0.0186)</b>	<b>0.0151 (0.0080)</b>
	vs	0.8997	0.2521	0.0441 (0.0589, 0.2016)	0.1487 (0.0664)	0.0153 (0.0156)
	vs + $\alpha$	<b>0.9009</b>	0.2519	0.0439 ( <b>0.0575</b> , 0.2016)	<b>0.1446 (0.0244)</b>	<b>0.0151 (0.0078)</b>
TTA	raw	0.9013	0.2458	0.0378 (0.0642, 0.1837)	0.1441 (0.0488)	0.0150 (0.0130)
	raw + $\alpha$	0.9025	<b>0.2456</b>	<b>0.0376 (0.0684, 0.1816)</b>	<b>0.1428 (0.0334)</b>	<b>0.0149 (0.0094)</b>
	ts	0.9012	0.2459	0.0379 (0.0646, 0.1837)	0.1448 (0.0553)	0.0150 (0.0143)
	ts + $\alpha$	0.9011	0.2458	0.0378 ( <b>0.0632</b> , 0.1839)	<b>0.1422 (0.0197)</b>	<b>0.0149 (0.0083)</b>
	vs	<b>0.9031</b>	0.2471	0.0392 (0.0671, 0.1862)	0.1458 (0.0598)	0.0151 (0.0149)
	vs + $\alpha$	0.9025	0.2470	0.0391 (0.0657, 0.1864)	<b>0.1428 (0.0247)</b>	<b>0.0149 (0.0082)</b>
	ms	0.9001	0.2489	0.0410 (0.0756, 0.1878)	0.1456 (0.0561)	0.0151 (0.0153)
	ms + $\alpha$	0.8991	0.2487	0.0407 (0.0750, 0.1873)	<b>0.1431 (0.0268)</b>	<b>0.0150 (0.0087)</b>

Table 2 shows a summary of each approach’s test set performance, where all of the metrics are unbiased or debiased versions we have derived. Overall, accuracy and the expected squared loss  $\widehat{L}_{sq}$  are roughly linked and present an advantage of TTA methods over the others. For absolute performance subtracting irreducible components, the epistemic loss  $\widehat{EL}$  seems a more meaningful measure. The substantial discrepancy between  $\widehat{L}_{sq}$  and  $\widehat{EL}$  (83% for *raw* classifier) implies that the actual classifier’s performance is much closer to the optimal one than expected from the accuracy and  $\widehat{L}_{sq}$ . Among the CPE calibration methods, temperature and vector scaling (ts and vs) consistently improve (decrease) calibration measure  $\widehat{CL}$  of original output (raw) for each of Raw, MCDO, and TTA predictions (Fig. 2a). However, the complementary metric  $\widehat{DL}$  is also affected and not necessarily improved in general. As for the effect of  $\alpha$ -calibration, Order-1 metrics for Raw predictions are not degraded (Table 2) as expected and slightly improved in the other two. The most significant improvement with  $\alpha$ -calibration is observed in order-2 metrics. Fig. 2b shows a distinct improvement in the reliability of inter-rater disagreement by  $\alpha$ -calibration. The improvement in the order-2 metrics is also consistently observed for both the expected loss  $\widehat{L}_{\phi}$  and calibration error  $\widehat{CE}_{\phi}$  of overall inter-rater disagreement ( $\phi = \phi^D$ ) and the mean of those for the class-wise disagreement metrics ( $\phi = \phi_*^D$ ), as shown in Table 2.

## 7 Conclusion

In this work, we have developed a framework to evaluate probabilistic classifiers under the situation with ground truth label uncertainty, accompanied with useful metrics that enjoyed unbiased or debiased properties. The framework also has been generalized to evaluate higher-order statistics, including inter-rater disagreement. Then, the importance of obtaining a better CPE distribution was highlighted and addressed with a newly devised calibration method called  $\alpha$ -calibration. Empirical evaluations with a real-world medical imaging application showed the interpretability of our uncertainty-aware metrics and the clear advantage of  $\alpha$ -calibration for predictions on inter-rater disagreements.



## Acknowledgement

IS was supported by JSPS KAKENHI Grant Number 20H04239 Japan.

## References

- [1] Murat Seckin Ayhan and Philipp Berens. Test-time data augmentation for estimation of heteroscedastic aleatoric uncertainty in deep neural networks. 2018.
- [2] Glenn W Brier. Verification of forecasts expressed in terms of probability. *Monthly weather review*, 78(1):1–3, 1950.
- [3] Jochen Bröcker. Estimating reliability and resolution of probability forecasts through decomposition of the empirical score. *Climate dynamics*, 39(3-4):655–667, 2012.
- [4] François Chollet et al. Keras. <https://keras.io>, 2015.
- [5] Morris H DeGroot and Stephen E Fienberg. The comparison and evaluation of forecasters. *Journal of the Royal Statistical Society: Series D (The Statistician)*, 32(1-2):12–22, 1983.
- [6] Armen Der Kiureghian and Ove Ditlevsen. Aleatory or epistemic? does it matter? *Structural safety*, 31(2): 105–112, 2009.
- [7] Christopher AT Ferro and Thomas E Fricker. A bias-corrected decomposition of the brier score. *Quarterly Journal of the Royal Meteorological Society*, 138(668):1954–1960, 2012.
- [8] Yarin Gal and Zoubin Ghahramani. Dropout as a bayesian approximation: Representing model uncertainty in deep learning. In *international conference on machine learning*, pages 1050–1059, 2016.
- [9] Tilmann Gneiting and Adrian E Raftery. Strictly proper scoring rules, prediction, and estimation. *Journal of the American statistical Association*, 102(477):359–378, 2007.
- [10] Chuan Guo, Geoff Pleiss, Yu Sun, and Kilian Q Weinberger. On calibration of modern neural networks. In *Proceedings of the 34th International Conference on Machine Learning-Volume 70*, pages 1321–1330. JMLR. org, 2017.
- [11] Kaiming He, Xiangyu Zhang, Shaoqing Ren, and Jian Sun. Deep residual learning for image recognition. In *Proceedings of the IEEE conference on computer vision and pattern recognition*, pages 770–778, 2016.
- [12] Wassily Hoeffding. A class of statistics with asymptotically normal distribution. In *Breakthroughs in Statistics*, pages 308–334. Springer, 1992.
- [13] Martin Holm Jensen, Dan Richter Jørgensen, Raluca Jalaboi, Mads Eiler Hansen, and Martin Aastrup Olsen. Improving uncertainty estimation in convolutional neural networks using inter-rater agreement. In *International Conference on Medical Image Computing and Computer-Assisted Intervention*, pages 540–548. Springer, 2019.
- [14] Taejong Joo, Uijung Chung, and Min-Gwan Seo. Being bayesian about categorical probability. *arXiv preprint arXiv:2002.07965*, 2020.
- [15] Alex Kendall and Yarin Gal. What uncertainties do we need in bayesian deep learning for computer vision? In *Advances in neural information processing systems*, pages 5574–5584, 2017.
- [16] Diederik P Kingma and Jimmy Ba. Adam: A method for stochastic optimization. *arXiv preprint arXiv:1412.6980*, 2014.
- [17] Meelis Kull and Peter Flach. Novel decompositions of proper scoring rules for classification: Score adjustment as precursor to calibration. In *Joint European Conference on Machine Learning and Knowledge Discovery in Databases*, pages 68–85. Springer, 2015.
- [18] Meelis Kull, Miquel Perello Nieto, Markus Kängsepp, Telmo Silva Filho, Hao Song, and Peter Flach. Beyond temperature scaling: Obtaining well-calibrated multi-class probabilities with dirichlet calibration. In *Advances in Neural Information Processing Systems*, pages 12295–12305, 2019.
- [19] Ananya Kumar, Percy S Liang, and Tengyu Ma. Verified uncertainty calibration. In *Advances in Neural Information Processing Systems*, pages 3787–3798, 2019.
- [20] Yann LeCun, Corinna Cortes, and CJ Burges. Mnist handwritten digit database. *ATT Labs [Online]*. Available: <http://yann.lecun.com/exdb/mnist>, 2, 2010.
- [21] Andrey Malinin and Mark Gales. Predictive uncertainty estimation via prior networks. In *Advances in Neural Information Processing Systems*, pages 7047–7058, 2018.

- 
- [22] Allan H Murphy. A new vector partition of the probability score. *Journal of applied Meteorology*, 12(4):595–600, 1973.
- [23] Mahdi Pakdaman Naeni, Gregory Cooper, and Milos Hauskrecht. Obtaining well calibrated probabilities using bayesian binning. In *Twenty-Ninth AAAI Conference on Artificial Intelligence*, 2015.
- [24] John Platt et al. Probabilistic outputs for support vector machines and comparisons to regularized likelihood methods. *Advances in large margin classifiers*, 10(3):61–74, 1999.
- [25] Maithra Raghu, Katy Blumer, Rory Sayres, Ziad Obermeyer, Robert Kleinberg, Sendhil Mullainathan, and Jon Kleinberg. Direct uncertainty prediction for medical second opinions. *arXiv preprint arXiv:1807.01771*, 2018.
- [26] Amir Rahimi, Amirreza Shaban, Ching-An Cheng, Byron Boots, and Richard Hartley. Intra order-preserving functions for calibration of multi-class neural networks. *arXiv preprint arXiv:2003.06820*, 2020.
- [27] Peter Sadowski and Pierre Baldi. Neural network regression with beta, dirichlet, and dirichlet-multinomial outputs. 2018.
- [28] Keiko Sasada, Noriko Yamamoto, Hiroki Masuda, Yoko Tanaka, Ayako Ishihara, Yasushi Takamatsu, Yutaka Yatomi, Waichiro Katsuda, Issei Sato, Hiroataka Matsui, et al. Inter-observer variance and the need for standardization in the morphological classification of myelodysplastic syndrome. *Leukemia research*, 69:54–59, 2018.
- [29] Robin Senge, Stefan Bösner, Krzysztof Dembczyński, Jörg Haasenritter, Oliver Hirsch, Norbert Donner-Banzhoff, and Eyke Hüllermeier. Reliable classification: Learning classifiers that distinguish aleatoric and epistemic uncertainty. *Information Sciences*, 255:16–29, 2014.
- [30] Murat Sensoy, Lance Kaplan, and Melih Kandemir. Evidential deep learning to quantify classification uncertainty. In *Advances in Neural Information Processing Systems*, pages 3179–3189, 2018.
- [31] Karen Simonyan and Andrew Zisserman. Very deep convolutional networks for large-scale image recognition. *arXiv preprint arXiv:1409.1556*, 2014.
- [32] David B Stephenson, Caio AS Coelho, and Ian T Jolliffe. Two extra components in the brier score decomposition. *Weather and Forecasting*, 23(4):752–757, 2008.
- [33] Mattias Teye, Hossein Azizpour, and Kevin Smith. Bayesian uncertainty estimation for batch normalized deep networks. In *International Conference on Machine Learning*, pages 4907–4916, 2018.
- [34] Juozas Vaicenavicius, David Widmann, Carl Andersson, Fredrik Lindsten, Jacob Roll, and Thomas B Schön. Evaluating model calibration in classification. *arXiv preprint arXiv:1902.06977*, 2019.
- [35] Guotai Wang, Wenqi Li, Michael Aertsen, Jan Deprest, Sébastien Ourselin, and Tom Vercauteren. Aleatoric uncertainty estimation with test-time augmentation for medical image segmentation with convolutional neural networks. *Neurocomputing*, 338:34–45, 2019.
- [36] David Widmann, Fredrik Lindsten, and Dave Zachariah. Calibration tests in multi-class classification: A unifying framework. In *Advances in Neural Information Processing Systems*, pages 12236–12246, 2019.
- [37] Bianca Zadrozny and Charles Elkan. Obtaining calibrated probability estimates from decision trees and naive bayesian classifiers. In *Icml*, volume 1, pages 609–616. Citeseer, 2001.
- [38] Bianca Zadrozny and Charles Elkan. Transforming classifier scores into accurate multiclass probability estimates. In *Proceedings of the eighth ACM SIGKDD international conference on Knowledge discovery and data mining*, pages 694–699, 2002.
- [39] Jize Zhang, Bhavya Kailkhura, and T Han. Mix-n-match: Ensemble and compositional methods for uncertainty calibration in deep learning. *arXiv preprint arXiv:2003.07329*, 2020.

## A Decompositions of proper losses

We mainly describe the proofs for proper loss decompositions introduced in section 2. Before that, we restate the definition of an expected loss  $L$ . Given a strictly proper loss  $\ell(Y, Z)$  for a label  $Y \in e^K$  and a prediction  $Z \in \Delta^{K-1}$ , accompanied with the divergence function  $d(Y, Z) := \ell(Y, Z) - \ell(Y, Y)$ , the expected loss  $L$  is defined as follows:

**Definition 4** (Expected loss).

$$L := \mathbb{E}[d(Y, Z)] \quad (18)$$

Note that for cases with  $\ell = \ell_{\text{sq}}$  or  $\ell_{\text{log}}$ , it satisfies  $\forall Y \in e^K, \ell(Y, Y) = 0$  and  $d(Y, Z) = \ell(Y, Z)$ . In these cases,  $L = \mathbb{E}[\ell(Y, Z)]$ .

### A.1 Decomposition of proper losses and calibration

As we have described in section 2.4, the expected loss  $L$  can be decomposed as follows:

**Theorem 1** (DeGroot and Fienberg [5]). The expectation of proper loss  $\ell$  is decomposed into non-negative terms as follows:

$$L = \text{CL} + \text{RL}, \quad \text{where} \quad \begin{cases} \text{CL} := \mathbb{E}[d(C, Z)], & \text{(Calibration Loss)} \\ \text{RL} := \mathbb{E}[d(Y, C)], & \text{(Refinement Loss)} \end{cases} \quad (19)$$

where a calibration map  $C := \mathbb{E}[Y|Z] \in \Delta^{K-1}$  is defined as in Def. 1.

*Proof.*

$$\begin{aligned} L &= \mathbb{E}[d(Y, Z)] \\ &= \mathbb{E}[\ell(Y, Z) - \ell(Y, Y)] \\ &= \mathbb{E}[\ell(Y, Z) - \ell(Y, C)] + \mathbb{E}[\ell(Y, C) - \ell(Y, Y)] \\ &= \mathbb{E}[\mathbb{E}[\ell(Y, Z) - \ell(Y, C)|Z]] + \mathbb{E}[d(Y, C)], \end{aligned}$$

where the second term equals to the RL term. For the first term, as we have defined  $\ell(q, Z) := \mathbb{E}_{Y \sim \text{Cat}(q)}[\ell(Y, Z)]$  when  $q \in \Delta^{K-1}$ , the subterms can be rewritten as follows:

$$\begin{aligned} \mathbb{E}[\ell(Y, Z)|Z] &= \mathbb{E}_{Y \sim \text{Cat}(\mathbb{E}[Y|Z])}[\ell(Y, Z)] = \ell(\mathbb{E}[Y|Z], Z) = \ell(C, Z), \\ \mathbb{E}[\ell(Y, C)|Z] &= \mathbb{E}_{Y \sim \text{Cat}(\mathbb{E}[Y|Z])}[\ell(Y, C)] = \ell(\mathbb{E}[Y|Z], C) = \ell(C, C). \end{aligned}$$

Hence, the first term equals to the CL term as follows:

$$\mathbb{E}[\mathbb{E}[\ell(Y, Z) - \ell(Y, C)|Z]] = \mathbb{E}[\mathbb{E}[\ell(C, Z) - \ell(C, C)|Z]] = \mathbb{E}[d(C, Z)].$$

□

Note that we have followed the terminology used in Kull and Flach [17]. The terms CL and RL are also referred to as reliability [3, 7] and sharpness [5].

### A.2 Decompositions of proper losses under label uncertainty

As we have described in section 2.4, if  $Y$  follows an instance-wise categorical distribution with a probability vector, *i.e.*,  $Y|X \sim \text{Cat}(Q)$ , where  $Q(X) \in \Delta^{K-1}$ ,  $L$  can be further decomposed as follows:

**Theorem 2** (Kull and Flach [17]). The expectation of proper loss  $\ell$  is decomposed into non-negative terms as follows:<sup>3</sup>

$$L = \text{EL} + \text{IL} = \underbrace{\text{CL} + \text{ERL}}_{\text{EL}} + \text{IL}, \quad (20)$$

$$\text{where} \quad \begin{cases} \text{EL} = \mathbb{E}[d(Q, Z)], & \text{(Epistemic Loss)} \\ \text{IL} = \mathbb{E}[d(Y, Q)], & \text{(Irreducible Loss)} \\ \text{ERL} = \mathbb{E}[d(Q, C)]. & \text{(Epistemic Refinement Loss)} \end{cases} \quad (21)$$

Note that the CL term is the same form as in equation (5).

<sup>3</sup>The original paper refers to the ERL term as grouping loss (GL).

*Proof.* We first prove the first equality.

$$\begin{aligned}
L &= \mathbb{E}[d(Y, Z)] \\
&= \mathbb{E}[\ell(Y, Z) - \ell(Y, Y)] \\
&= \mathbb{E}[\ell(Y, Z) - \ell(Y, Q)] + \mathbb{E}[\ell(Y, Q) - \ell(Y, Y)] \\
&= \mathbb{E}[\mathbb{E}[\ell(Y, Z) - \ell(Y, Q)|Q]] + \mathbb{E}[d(Y, Q)],
\end{aligned}$$

where the second term is IL. As similar to the proof of Theorem 1, the following relations hold:

$$\begin{aligned}
\mathbb{E}[\ell(Y, Z)|Q] &= \mathbb{E}_{Y \sim Q}[\ell(Y, Z)|Q] = \mathbb{E}[\ell(Q, Z)|Q], \\
\mathbb{E}[\ell(Y, Q)|Q] &= \mathbb{E}_{Y \sim Q}[\ell(Y, Q)|Q] = \mathbb{E}[\ell(Q, Q)|Q].
\end{aligned}$$

Therefore, the first term turns out to be EL as follows:

$$\mathbb{E}[\mathbb{E}[\ell(Y, Z) - \ell(Y, Q)|Q]] = \mathbb{E}[\mathbb{E}[\ell(Q, Z) - \ell(Q, Q)|Q]] = \mathbb{E}[d(Q, Z)].$$

This term is further decomposed as follows:

$$\begin{aligned}
\mathbb{E}[d(Q, Z)] &= \mathbb{E}[\ell(Q, Z) - \ell(Q, C)] + \mathbb{E}[\ell(Q, C) - \ell(Q, Q)] \\
&= \mathbb{E}[\mathbb{E}[\ell(Q, Z) - \ell(Q, C)|Z]] + \mathbb{E}[d(Q, C)],
\end{aligned}$$

where the second term is ERL. To show that the first term is CL, we have to prove the following results:

$$\begin{aligned}
\mathbb{E}[\ell(Q, Z)|Z] &= \mathbb{E}[\ell(C, Z)|Z], \\
\mathbb{E}[\ell(Q, C)|Z] &= \mathbb{E}[\ell(C, C)|Z].
\end{aligned}$$

As these are proven with the same procedure, we only show the proof for the first equality.

$$\begin{aligned}
\mathbb{E}[\ell(Q, Z)|Z] &= \mathbb{E}[\mathbb{E}_{Y \sim Q} \ell(Y, Z)|Z] \\
&= \mathbb{E}\left[\sum_k \ell(Y_k, Z) Q_k | Z\right] \\
&= \mathbb{E}\left[\sum_k \ell(Y_k, Z) \mathbb{E}[Y|Z]_k | Z\right] \\
&= \mathbb{E}\left[\sum_k \ell(Y_k, Z) C_k | Z\right] \\
&= \mathbb{E}[\mathbb{E}_{Y \sim C}[\ell(Y, Z)]|Z] = \mathbb{E}[\ell(C, Z)|Z].
\end{aligned}$$

□

Theorems and proofs for more generalized decompositions are found in Kull and Flach [17].

## B Evaluation of class probability estimates with label histograms (details)

Details and proofs of the statements made in section 3 are described.

### B.1 Unbiased Estimators of $L_{sq}$

The proposition below is a restatement of Prop. 1.

**Proposition 5** (Unbiased estimator of expected squared loss). The following estimator of  $L_{sq}$  is unbiased.

$$\widehat{L}_{sq} := \frac{1}{W} \sum_{i=1}^N w_i \sum_{k=1}^K [(\widehat{\mu}_{ik} - z_{ik})^2 + \widehat{\mu}_{ik}(1 - \widehat{\mu}_{ik})], \quad (22)$$

where  $\widehat{\mu}_{ik} := y_{ik}/n_i$ ,  $w_i \geq 0$ , and  $W := \sum_{i=1}^N w_i$ .

*Proof.* We begin with the following plugin estimator of  $L_{sq}$  with an instance  $i$ :

$$\widetilde{L}_{sq,i} := \sum_k \frac{1}{n_i} \sum_{j=1}^{n_i} (y_{ik}^{(j)} - z_{ik})^2. \quad (23)$$

By taking an expectation with respect to  $y_{ik}$  and  $z_{ik}$ ,

$$\mathbb{E}[\tilde{L}_{\text{sq},i}] = \frac{1}{n_i} \sum_{j=1}^{n_i} \sum_k \mathbb{E}[(y_{ik}^{(j)} - z_{ik})^2] = \sum_k \mathbb{E}[(Y_k - Z_k)^2] = \mathbb{E}[\|Y - Z\|^2] = L_{\text{sq}}.$$

Therefore,  $\tilde{L}_{\text{sq},i}$  is an unbiased estimator of  $L_{\text{sq}}$ . Intuitively, an estimator combined with  $N$  instances is expected to have a lower variance than that with a single instance. A linear combination of  $\tilde{L}_{\text{sq},1}, \dots, \tilde{L}_{\text{sq},N}$  is also an unbiased estimator as follows:

$$\frac{1}{W} \mathbb{E}\left[\sum_i w_i \tilde{L}_{\text{sq},i}\right] = \frac{1}{W} \sum_i w_i \mathbb{E}[\tilde{L}_{\text{sq},i}] = L_{\text{sq}},$$

where  $\sum_i w_i \geq 0$ ,  $W := \sum_i w_i$ . The proof completes by transforming  $\tilde{L}_{\text{sq},i}$  as follows:

$$\tilde{L}_{\text{sq},i} = \sum_k \frac{1}{n_i} \sum_{j=1}^{n_i} (y_{ik}^{(j)} - 2y_{ik}^{(j)} z_{ik} + z_{ik}^2) = \sum_k (\hat{\mu}_{ik} - 2\hat{\mu}_{ik} z_{ik} + z_{ik}^2) = \sum_k \hat{\mu}_{ik}(1 - \hat{\mu}_{ik}) + (\hat{\mu}_{ik} - z_{ik})^2.$$

□

**Determination of weights  $w$**  For the undetermined weights  $w_1, \dots, w_N$ , we have argued that the optimal weights would be constant when the numbers of annotators  $n_1, \dots, n_N$  were constant. As we assume that each of an instance  $i$  follows an independent categorical distribution with a parameter  $Q_i \in \Delta^{K-1}$ , the variance of  $\hat{L}_{\text{sq},k}$  is decomposed as follows:

$$\mathbb{V}[\hat{L}_{\text{sq},k}] = \sum_{i=1}^N \left(\frac{w_i}{W}\right)^2 \mathbb{V}[\hat{L}_{\text{sq},ik}]. \quad (24)$$

Thus, if  $n_i$  is constant for all the instance, the optimal weights are found as follows:

$$\min_{\mathbf{w}'} \sum_{i=1}^N w_i'^2 \quad s.t. \quad \sum_{i=1}^N w_i' = 1, \quad \forall i, w_i' \geq 0, \quad (25)$$

By taking a derivative with respect to  $\mathbf{w}'$  of  $\sum_{i=1}^N w_i'^2 + \lambda(\sum_{i=1}^N w_i' - 1)$ , the solution is  $\forall i, w_i' = 1/N$ .

For cases with varying numbers of annotators per instance, it is not straightforward to determine the optimal weights. From a standard result of variance formulas, the variance of  $\hat{L}_{\text{sq}}$  is further decomposed as follows:

$$\begin{aligned} \mathbb{V}[\hat{L}_{\text{sq},ik}] &:= \mathbb{E}[\mathbb{V}[\hat{L}_{\text{sq},ik} | X_i]] + \mathbb{V}[\mathbb{E}[\hat{L}_{\text{sq},ik} | X_i]] \\ &= \frac{1}{n_i} \mathbb{E}[\sigma_{\text{sq},k}^2(X)] + \mathbb{V}[\mu_{\text{sq},k}(X)], \end{aligned}$$

where  $\mu_{\text{sq},k}(X) := \mathbb{E}[(Y_k - Z_k)^2 | X]$  and  $\sigma_{\text{sq},k}^2(X) := \mathbb{V}[(Y_k - Z_k)^2 | X]$ . Therefore, the optimal weights depend on the ratio of the first and the second terms. If the first term is negligible compared to the second term, using the constant weights regardless of  $n_i$  would be optimal. In contrast, if the first term is dominant,  $w_i \propto n_i$  would be optimal. However, the ratio of the two terms depend on the dataset and is not determined a priori. In this work, we have used  $w_i = 1$ .

## B.2 Unbiased Estimators of EL

We restate the plugin estimator of the EL as follows:

**Definition 5** (Plugin estimator of EL).

$$\widetilde{\text{EL}} := \frac{1}{N} \sum_{i=1}^N \sum_{k=1}^K (\hat{\mu}_{ik} - z_{ik})^2. \quad (26)$$

The proposition below is a restatement of Prop. 2.

**Proposition 6** (Unbiased estimator of EL). The following estimator of EL is unbiased.

$$\widehat{\text{EL}} := \widetilde{\text{EL}} - \frac{1}{N} \sum_i \sum_k \frac{1}{n_i - 1} \hat{\mu}_{ik}(1 - \hat{\mu}_{ik}). \quad (27)$$

*Proof.* The term EL is decomposed as  $EL = \sum_k EL_k$ , where

$$EL_k = \mathbb{E}[(Q_k - Z_k)^2] = \mathbb{E}[Q_k^2] - 2\mathbb{E}[Q_k Z_k] + \mathbb{E}[Z_k^2].$$

As for the terms in the plugin estimator  $\widetilde{EL} = \sum_k \widetilde{EL}_k$ , we can show that

$$\begin{aligned} \mathbb{E}[\widehat{\mu}_{ik} z_{ik}] &= \frac{1}{n_i} n_i \mathbb{E}[Q_k Z_k] = \mathbb{E}[Q_k Z_k], \\ \mathbb{E}[z_{ik}^2] &= \mathbb{E}[Z_k^2]. \end{aligned}$$

The bias of  $\widetilde{EL}_k$  comes from  $\widehat{\mu}_{ik}^2$ , that corresponds to  $\mathbb{E}[Q_k^2]$  term. We can replace  $\widehat{\mu}_{ik}^2$  by an unbiased estimator as follows:

$$\widehat{\mu}_{ik}^2 \rightarrow \frac{1}{n_i(n_i - 1)} \sum_{j=1}^{n_i} \sum_{j'=1: j' \neq j}^{n_i} y_{ik}^{(j)} y_{ik}^{(j')}, \quad (28)$$

where an expectation of each of the summand of *r.h.s.* is  $\mathbb{E}[Q_k^2]$ , hence that of *r.h.s.* is also be  $\mathbb{E}[Q_k^2]$ . Consequently, the difference of the plugin estimator  $\widetilde{EL}_k$  and the unbiased estimator  $\widehat{EL}_k$  is calculated as follows:

$$\begin{aligned} \widetilde{EL}_k - \widehat{EL}_k &= \frac{1}{N} \sum_i \left[ \widehat{\mu}_i^2 - \frac{1}{n_i(n_i - 1)} \sum_{j=1}^{n_i} \sum_{j'=1: j' \neq j}^{n_i} y_{ik}^{(j)} y_{ik}^{(j')} \right] \\ &= \frac{1}{N} \sum_i \left\{ \widehat{\mu}_i^2 - \frac{1}{n_i(n_i - 1)} \left[ \left( \sum_{j=1}^{n_i} y_{ik}^{(j)} \right)^2 - \sum_{j=1}^{n_i} y_{ik}^{(j)} \right] \right\} \\ &= \frac{1}{N} \sum_i \left\{ \widehat{\mu}_i^2 - \frac{1}{n_i(n_i - 1)} \left( n_i^2 \widehat{\mu}_{ik}^2 - n_i \widehat{\mu}_{ik} \right) \right\} \\ &= \frac{1}{N} \sum_i \frac{1}{n_i - 1} \widehat{\mu}_{ik} (1 - \widehat{\mu}_{ik}). \end{aligned}$$

□

### B.3 Debiased Estimators of CL

**Definition 6** (Plugin estimator of CL).

$$\widetilde{CL}_{kb}(\mathcal{B}_k) := \frac{|I_{kb}|}{N} (\bar{c}_{kb} - \bar{z}_{kb})^2, \quad \text{where} \quad \bar{c}_{kb} := \frac{\sum_{i \in I_{kb}} \widehat{\mu}_{ik}}{|I_{kb}|}, \quad \bar{z}_{kb} := \frac{\sum_{i \in I_{kb}} z_{ik}}{|I_{kb}|}, \quad (29)$$

where  $I_{kb} := \{i \mid z_{ik} \in \mathcal{B}_{kb}\}$  denotes an index set of  $b$ -th bin and  $\mathcal{B}_{kb} := [\zeta_{kb}, \zeta_{kb+1})$  is a  $b$ -th interval of the binning scheme  $\mathcal{B}_k$ .

The proposition below is a restatement of Prop. 3.

**Proposition 7** (Debiased estimator of  $CL_{kb}$ ). The plugin estimator of  $CL_{kb}$  is debiased with the following estimator:

$$\widehat{CL}_{kb}(\mathcal{B}_k) := \widetilde{CL}_{kb}(\mathcal{B}_k) - \frac{|I_{kb}|}{N} \frac{\bar{\sigma}_{kb}^2}{|I_{kb}| - 1}, \quad \text{where} \quad \bar{\sigma}_{kb}^2 := \frac{1}{|I_{kb}|} \sum_{i \in I_{kb}} \widehat{\mu}_{ik}^2 - \left( \frac{1}{|I_{kb}|} \sum_{i \in I_{kb}} \widehat{\mu}_{ik} \right)^2. \quad (30)$$

*Proof.* The bias of the plugin estimator  $\widetilde{CL}_{kb}$  is explained in a similar manner as in the case of  $\widetilde{EL}_k$ . Concretely, a bias of the term  $\bar{c}_{kb}^2$  for an estimation of  $C_{kb}^2$  can be reduced with a following replacement:

$$\bar{c}_{kb}^2 \rightarrow \frac{1}{|I_{kb}|(|I_{kb}| - 1)} \sum_{i \in I_{kb}} \sum_{i' \in I_{kb}: i' \neq i} \widehat{\mu}_{ik} \widehat{\mu}_{i'k}. \quad (31)$$

Note that the *r.h.s.* term is only defined for the bin with  $|I_{kb}| > 1$ . In this case, a conditional expectation of the term is as follows:

$$\begin{aligned} \mathbb{E}\left[\frac{|I_{kb}|}{N} \cdot r.h.s., |I_{kb}| > 1\right] &= \sum_{m=2}^N \frac{\mathbb{E}[|I_{kb}| = m]m}{N} \frac{1}{m(m-1)} \sum_{i \in I_{kb}} \sum_{i' \in I_{kb}: i' \neq i} \mathbb{E}[\widehat{\mu}_{ik} \widehat{\mu}_{i'k} | |I_{kb}| = m] \\ &= \sum_{m=2}^N \frac{\mathbb{E}[|I_{kb}| = m]m}{N} \bar{C}_{kb}^2 = \frac{\mathbb{E}[|I_{kb}| | |I_{kb}| > 1]}{N} \bar{C}_{kb}^2 \\ &= (\mathbb{E}[Z_k \in \mathcal{B}_{kb}] - \eta_{kb}) \bar{C}_{kb}^2, \end{aligned}$$

where  $\eta_{kb} = \mathbb{E}[I_{kb} \leq 1]/N$ , which can be reduced by increasing  $N$  relative to the bin size. When we use the *r.h.s.* = 0 for  $|I_{kb}| \leq 1$ ,  $\eta_{kb} \bar{C}_{kb}^2$  is a remained bias term after the replacement in equation (31). When we define an estimator  $\widehat{CL}_{kb}$  as a modified  $\widetilde{CL}_{kb}$  that has been applied the replacement (31), a debiasing amount of the bias with the modification is calculated as follows:

$$\begin{aligned} \widetilde{CL}_{kb} - \widehat{CL}_{kb} &= \frac{|I_{kb}|}{N} \left\{ \bar{c}_{kb}^2 - \frac{1}{|I_{kb}|(|I_{kb}| - 1)} \sum_{i \in I_{kb}} \sum_{i' \in I_{kb}: i' \neq i} \widehat{\mu}_{ik} \widehat{\mu}_{i'k} \right\} \\ &= \frac{|I_{kb}|}{N} \left\{ \bar{c}_{kb}^2 - \frac{1}{|I_{kb}|(|I_{kb}| - 1)} \left[ (|I_{kb}| \bar{c}_{kb})^2 - \sum_{i \in I_{kb}} \widehat{\mu}_{ik}^2 \right] \right\} \\ &= \frac{|I_{kb}|}{N} \left\{ \frac{1}{|I_{kb}| - 1} \left[ \frac{1}{|I_{kb}|} \sum_{i \in I_{kb}} \widehat{\mu}_{ik}^2 - \bar{c}_{kb}^2 \right] \right\} = \frac{|I_{kb}|}{N} \frac{\bar{\sigma}_{kb}^2}{|I_{kb}| - 1}. \end{aligned}$$

□

Note that as we mentioned in the proof, the bin-wise debiasing cannot be applied for the bins with  $|I_{kb}| \leq 1$ . We use 0 for the estimators with such bins. For single-labeled data, the remaining bias from this limitation is also analyzed in the literature [7].

#### B.4 Definition and estimators of dispersion loss

The proposition below is a restatement of Prop. 4.

**Proposition 8** (Non-negativity of dispersion loss). Given a binning scheme  $\mathcal{B}$ , a dispersion loss for class  $k$  is decomposed into bin-wise components, where each term takes a non-negative value:

$$DL_k(\mathcal{B}) := EL_k - CL_k(\mathcal{B}) = \sum_b DL_{kb}(\mathcal{B}), \quad (32)$$

$$DL_{kb}(\mathcal{B}) := \mathbb{E}[\mathbb{E}\{[(Q_k - \bar{C}_{kb}) - (Z_k - \bar{Z}_{kb})]^2 | Z_k \in \mathcal{B}_{kb}\}] \geq 0. \quad (33)$$

*Proof.* From the definition of  $DL_k(\mathcal{B})$ ,

$$\begin{aligned} DL_k(\mathcal{B}) &:= EL_k - CL_k(\mathcal{B}) \\ &= \mathbb{E}[(Q_k - Z_k)^2] - \sum_b \mathbb{E}[\mathbb{E}[(\bar{C}_{kb} - \bar{Z}_{kb})^2 | Z_k \in \mathcal{B}_{kb}]] \\ &= \sum_b \mathbb{E}[\mathbb{E}[(Q_k - Z_k)^2 - (\bar{C}_{kb} - \bar{Z}_{kb})^2 | Z_k \in \mathcal{B}_{kb}]] \\ &= \sum_b DL_{kb}(\mathcal{B}), \end{aligned}$$

$$\text{where } DL_{kb}(\mathcal{B}) := \mathbb{E}[\mathbb{E}[(Q_k - Z_k)^2 - (\bar{C}_{kb} - \bar{Z}_{kb})^2 | Z_k \in \mathcal{B}_{kb}]].$$

By noting that  $\bar{C}_{kb} - \bar{Z}_{kb} = \mathbb{E}[Q_k - Z_k | Z_k \in \mathcal{B}_{kb}]$ , the last term is further transformed as follows:

$$\begin{aligned} DL_{kb}(\mathcal{B}) &= \mathbb{E}[\mathbb{E}[(Q_k - Z_k)^2 - (\bar{C}_{kb} - \bar{Z}_{kb})^2 | Z_k \in \mathcal{B}_{kb}]] \\ &= \mathbb{E}[\mathbb{E}[(Q_k - Z_k)^2 - 2(Q_k - Z_k)(\bar{C}_{kb} - \bar{Z}_{kb}) + (\bar{C}_{kb} - \bar{Z}_{kb})^2 | Z_k \in \mathcal{B}_{kb}]] \\ &= \mathbb{E}[\mathbb{E}\{[(Q_k - Z_k) - (\bar{C}_{kb} - \bar{Z}_{kb})]^2 | Z_k \in \mathcal{B}_{kb}\}] \\ &= \mathbb{E}[\mathbb{E}\{[(Q_k - \bar{C}_{kb}) - (Z_k - \bar{Z}_{kb})]^2 | Z_k \in \mathcal{B}_{kb}\}]. \end{aligned}$$

Then, the last term is apparently  $\geq 0$ .  $\square$

By using the plugin and the debiased estimators of EL and CL, those estimators of DL are defined as follows:

**Definition 7** (Plugin / debiased estimators of dispersion loss).

$$\widetilde{\text{DL}}_{kb}(\mathcal{B}) = \frac{1}{N} \sum_{i \in I_{kb}} \{(\widehat{\mu}_{ik} - \bar{c}_{kb}) - (z_{ik} - \bar{z}_{kb})\}^2, \quad (34)$$

$$\widehat{\text{DL}}_{kb}(\mathcal{B}) = \widetilde{\text{DL}}_{kb}(\mathcal{B}) - \frac{1}{N} \sum_{i \in I_{kb}} \left( \frac{1}{n_i - 1} \widehat{\mu}_{ik}(1 - \widehat{\mu}_{ik}) - \frac{\bar{\sigma}_{kb}^2}{|I_{kb}| - 1} \right). \quad (35)$$

### B.5 Experimental details for the debiasing effects of CL and DL terms

The details of the experimental setup and results in section 3.4 are described. As shown in Fig. 1, we compare the plugin and debiased estimators of CL and DL for ideal predictors and synthetic label histograms. The number of instances varies from 100 to 10,000, and the number of annotators per instance is 2 or 5. For each experiment, each instance's positive class probability is uniformly generated on a unit interval  $[0, 1]$ . A label histogram for each instance is generated in an i.i.d. manner following the Binomial distribution with the corresponding probability. The predictor is assumed to know the correct instance-wise class probability so that both of CL and DL be zero. For a binning scheme  $\mathcal{B}$  of the estimators, we adopt 15 equally-spaced binning, which is regularly used to evaluate calibration errors [10].

For each experiment, ten replicates are generated, and the empirical mean and the 90% confidence intervals of the mean values are plotted for all the estimators. As shown in Fig. 1, the debiased estimators:  $\widehat{\text{CL}}$  and  $\widehat{\text{DL}}$  significantly reduce biases of the plugin estimators:  $\widetilde{\text{CL}}$  and  $\widetilde{\text{DL}}$ , even in the cases with two annotators. The bias of the plugin estimator  $\widetilde{\text{CL}}$  decreases as the number of instances gets large. In contrast, that of the plugin estimator  $\widetilde{\text{DL}}$  remains steady for instance size, which is expected from the form of the bias term in equation (35).

## C Evaluation of higher-order statistics (details)

The details and proofs for the statements in section 4 are described. Let  $X \in \mathcal{X}$  be an input feature and  $\{Y^{(j)} \in e^K\}_{j=1}^n$  be  $n$  distinct labels for the same instance. We define a symmetric categorical statistics  $\phi : e^{K \times n} \rightarrow e^M$  ( $M \geq 2$ ) for the  $n$  labels. For the case of  $M = 2$ ,  $\phi$  can be equivalently represented as  $\phi : e^{K \times n} \rightarrow \{0, 1\}$ , and we use this definition for the successive discussion. In our experiments, we particularly focus on a disagreement between paired labels  $\phi^D = \mathbb{I}[Y^{(1)} \neq Y^{(2)}]$  and a class-wise variant of that  $\phi^{Dk} := \mathbb{I}[Y_k^{(1)} \neq Y_k^{(2)}]$  as predictive targets.

Consider a probability prediction  $\varphi : \mathcal{X} \rightarrow [0, 1]$  for statistics  $\phi : e^{K \times n} \rightarrow \{0, 1\}$ , a strictly proper loss  $\ell : \{0, 1\} \times [0, 1] \rightarrow \mathbb{R}$  encourages  $\varphi(X)$  to approach the right probability  $P(\phi(Y^{(1)}, \dots, Y^{(n)})|X)$  in expectation. We use (one dimensional) squared loss  $\ell(\phi, \varphi) = (\phi - \varphi)^2$  in our evaluation. The expected loss is as follows:

**Definition 8** (Expected squared loss for  $\phi$  and  $\varphi$ ).

$$L_\phi := \mathbb{E}[(\phi - \varphi)^2], \quad (36)$$

where the expectation is taken over the random variables  $X$  and  $Y^{(1)}, \dots, Y^{(n)}$ .

Note that  $L_\phi$  for an empirical distribution is equivalent to Brier score of  $\phi$  and  $\varphi$ . A decomposition of  $L_\phi$  into  $\text{CL}_\phi$  and  $\text{RL}_\phi$  is readily available by applying Theorem 1.

$$L_\phi := \mathbb{E}[(\phi - \varphi)^2] = \underbrace{\mathbb{E}[(\mathbb{E}[\phi|\varphi] - \varphi)^2]}_{\text{CL}_\phi} + \underbrace{\mathbb{E}[(\phi - \mathbb{E}[\phi|\varphi])^2]}_{\text{RL}_\phi}. \quad (37)$$

We will derive the estimators of  $L_\phi$  and  $\text{CL}_\phi$  as evaluation metrics. However, the number of labels per instance is  $n_i \geq n$  in general<sup>4</sup>, which results in multiple inconsistent statistics  $\phi$  for the same instance. The problem can be solved with similar treatments as in the evaluation of CPEs.

As we stated in section 4, an unbiased estimator of the mean statistics for each instance  $\mu_{\phi,i} := \mathbb{E}[\phi|X = x_i]$  is a useful building block in the estimation of  $L_\phi$  and  $\text{CL}_\phi$ . Recall that we assume a conditional independence of an arbitrary number of labels given an input feature, i.e.,  $Y^{(1)}, \dots, Y^{(n_i)}|X \underset{i.i.d.}{\sim} \text{Cat}(Q(X))$ ,  $\mu_{\phi,i}$  is estimated as follows:

<sup>4</sup>We omit an instance with  $n_i < n$  where  $\phi$  cannot be calculated with distinct  $n$  labels.



**Theorem 3** (Unbiased estimator of  $\mu_{\phi,i}$ ). For an instance  $i$  with  $n_i$  labels obtained in a conditional i.i.d. manner, an unbiased estimator of the conditional mean  $\mu_{\phi,i}$  is given as follows:

$$\hat{\mu}_{\phi,i} := \binom{n_i}{n}^{-1} \sum_{j \in \text{Comb}(n_i, n)} \phi(y_i^{(j_1)}, \dots, y_i^{(j_n)}), \quad (38)$$

where  $\text{Comb}(n_i, n)$  denotes the distinct subset of size  $n$  drawn from  $\{1, \dots, n_i\}$  without replacement.

*Proof.* This is directly followed from the fact that  $\hat{\mu}_{\phi,i}$  is a U-statistic of  $n$ -sample symmetric kernel function  $\phi$  [12].  $\square$

### C.1 Unbiased estimator of $L_\phi$

**Theorem 4** (Unbiased estimator of  $L_\phi$ ). The following estimator is an unbiased estimator of  $L_\phi$ .

$$\hat{L}_\phi := \frac{1}{N} \sum_i \hat{L}_{\phi,i}, \quad \text{where} \quad \hat{L}_{\phi,i} := \binom{n_i}{n}^{-1} \sum_{j \in \text{Comb}(n_i, n)} \left( \phi(y_i^{(j_1)}, \dots, y_i^{(j_n)}) - \varphi_i \right)^2. \quad (39)$$

*Proof.* We first confirm that, for each random variables  $\phi(y_i^{(1)}, \dots, y_i^{(n)})$  and  $\varphi_i$  of sample  $i$ ,

$$\mathbb{E}[f(y_i^{(1)}, \dots, y_i^{(n)}; \varphi_i)] = L_\phi, \quad \text{where} \quad f(y_i^{(1)}, \dots, y_i^{(n)}; \varphi_i) := \left( \phi(y_i^{(1)}, \dots, y_i^{(n)}) - \varphi_i \right)^2,$$

satisfies by definition. As  $f$  is an  $n$ -sample symmetric kernel of variables  $y_i^{(1)}, \dots, y_i^{(n)}$ ,  $\hat{L}_{\phi,i}$  is a U-statistic [12] of the kernel given  $\varphi_i$  and also an unbiased estimator of  $L_\phi$  as follows:

$$\mathbb{E}[\hat{L}_{\phi,i}] = \mathbb{E}[\mathbb{E}[\hat{L}_{\phi,i} | \varphi_i]] = \mathbb{E}[\mathbb{E}[f(y_i^{(1)}, \dots, y_i^{(n)}; \varphi_i) | \varphi_i]] = L_\phi. \quad (40)$$

Hence

$$\mathbb{E}[\hat{L}_\phi] = \frac{1}{N} \sum_{i=1}^N \mathbb{E}[\hat{L}_{\phi,i}] = L_\phi. \quad \square$$

### C.2 Debiased estimator of $\text{CL}_\phi(\mathcal{B})$

Following the same discussion as the  $\text{CL}(\mathcal{B})$  term of CPEs, we also consider a binning based approximation of  $\text{CL}_\phi$  stratified with a binning scheme  $\mathcal{B}$  for predictive probability  $\varphi \in [0, 1]$ . Then, the plugin estimator of  $\text{CL}_\phi(\mathcal{B})$  is defined as follows:

**Definition 9** (Plugin estimator of  $\text{CL}_\phi$ ).

$$\widetilde{\text{CL}}_\phi(\mathcal{B}) := \sum_{b=1}^B \widetilde{\text{CL}}_{\phi,b}(\mathcal{B}), \quad (41)$$

$$\text{where} \quad \widetilde{\text{CL}}_{\phi,b}(\mathcal{B}) := \frac{|I_{\phi,b}|}{N} (\bar{c}_{\phi,b} - \bar{\varphi}_b)^2, \quad \bar{c}_{\phi,b} := \frac{\sum_{i \in I_{\phi,b}} \hat{\mu}_{\phi,i}}{|I_{\phi,b}|}, \quad \bar{\varphi}_b := \frac{\sum_{i \in I_{\phi,b}} \varphi_i}{|I_{\phi,b}|}. \quad (42)$$

We again improve the plugin estimator with the following debiased estimator  $\widehat{\text{CL}}_{\phi,b}(\mathcal{B})$ :

**Corollary 1** (Debiased estimator of  $\text{CL}_{\phi,b}$ ). A plugin estimator  $\widetilde{\text{CL}}_{\phi,b}(\mathcal{B})$  of  $\text{CL}_{\phi,b}(\mathcal{B})$  is debiased to  $\widehat{\text{CL}}_{\phi,b}(\mathcal{B})$  with a correction term as follows:

$$\widehat{\text{CL}}_{\phi,b}(\mathcal{B}) := \widetilde{\text{CL}}_{\phi,b}(\mathcal{B}) - \frac{|I_{\phi,b}|}{N} \frac{\bar{\sigma}_{\phi,b}^2}{|I_{\phi,b}| - 1}, \quad (43)$$

$$\text{where} \quad \bar{\sigma}_{\phi,b}^2 := \frac{1}{|I_{\phi,b}|} \sum_{i \in I_{\phi,b}} \hat{\mu}_{\phi,i}^2 - \left( \frac{1}{|I_{\phi,b}|} \sum_{i \in I_{\phi,b}} \hat{\mu}_{\phi,i} \right)^2. \quad (44)$$

Note that the estimator is only available for bins with  $|I_{\phi,b}| \geq 2$ .

*Proof.* The proof follows a similar reasoning to Prop. 7. We reduce the bias introduced with the term  $\bar{c}_{\phi,b}^2$  by replacing the term with unbiased one for  $\bar{C}_{\phi,b}^2 = \mathbb{E}[\phi|\varphi \in \mathcal{B}_b]^2$  as follows:

$$\bar{c}_{\phi,b}^2 \rightarrow \frac{1}{|I_{\phi,b}|(|I_{\phi,b}| - 1)} \sum_{i \in I_{\phi,b}} \sum_{i' \in I_{\phi,b}: i' \neq i} \hat{\mu}_{\phi,i} \hat{\mu}_{\phi,i'},$$

where  $\hat{\mu}_{\phi,i}$  is defined in equation (38). An improvement with the debiased estimator  $\widetilde{\text{CL}}_{\phi,b} - \widehat{\text{CL}}_{\phi,b}$  is also calculated with the same manner as in Prop. 7.  $\square$

## D Post-hoc uncertainty calibration methods (details)

### D.1 Summary of CPE calibration methods based on linear transformations

We summarize the CPE calibration methods based on linear transformations, which are used in our experiments. Denote  $z' = \text{softmax}(u') \in \Delta^{K-1}$  as the original CPE and  $u' \in \mathbb{R}^K$  as the logit vector. The common framework of a linear-type CPE calibration is given as follows:

$$u = Wu' + b, \quad (45)$$

$$z = \text{softmax}(u), \quad (46)$$

where  $z \in \Delta^{K-1}$  is a CPE after calibration,  $u$  is a transformed logit, and  $M \in \mathbb{R}^{K \times K}$  and  $b \in \mathbb{R}^K$  are coefficients that are learned from validation data. This general form is referred to as matrix scaling in the literature [10, 18]. Vector scaling is a constrained version of the matrix scaling such as  $W = \text{diag}(v)$ ,  $v \in \mathbb{R}^K$ . A variant with further constraint  $v = 1/t$ ,  $t \in \mathbb{R}$ ,  $b = 0$  is called temperature scaling. As temperature scaling does not change the order of vector elements between  $u$  and  $u'$ , it does not change the maximum predictive class of an instance and hence also an accuracy. For vector and matrix scaling, the regularization of parameters is known to be required. For vector scaling, an L2 regularization of an intercept vector  $b$  is commonly used as follows:

$$\Omega_{\text{L2}}(b) := \lambda_b \frac{1}{K} \sum_k b_k^2. \quad (47)$$

For matrix scaling, the following off-diagonal and intercept regularization (ODIR) [18] is also proposed.

$$\Omega_{\text{ODIR}}(W, b) := \lambda_w \frac{1}{K(K-1)} \sum_{k \neq k'} W_{kk'}^2 + \lambda_b \frac{1}{K} \sum_k b_k^2. \quad (48)$$

### D.2 Details of $\alpha$ -calibration

The  $\alpha$ -calibration infers CPE distribution for trained neural networks that only output CPEs as a point estimate  $z \in \Delta^{K-1}$ . We use the Dirichlet distribution  $\text{Dir}(z|\alpha)$  as a model for a distribution over CPEs, where only  $\alpha_0 = \sum_k \alpha_k$  is optimized while the expectation of CPEs  $\mathbb{E}[z] = \alpha/\alpha_0$  is unchanged. This treatment prevents the degradation of CPEs regardless of potential model misspecification for label histograms, as similar to temperature scaling preserving accuracy.

An  $\alpha_0$  is parametrized with a full connection layer whose input vector is given from a feature layer behind the last softmax layer. An output vector of  $\alpha$ -calibration will be  $\alpha = \alpha_0 z'$ , where  $z'$  denotes the original CPE output,  $\alpha_0 = \exp(Wu + b)$ , and  $u$  denotes an output vector of the feature layer. For a loss function to be minimized, we use a negative log-likelihood of an observed label histogram  $y$  with respect to the Dirichlet multinomial distribution  $\text{DirMult}(y|\alpha)$ . We also use a regularization term  $\lambda_\alpha (\log \alpha_0)^2$  for stabilization purpose, which penalizes the deviation from  $\alpha_0 = 1$  to both directions towards extreme concentrations of the mass on  $\delta(z = \mathbb{E}[z])$  or  $\sum_k \delta(z = e_k) \mathbb{E}[z_k]$ , that correspond to purely aleatoric or purely epistemic uncertainty, respectively. We employ  $\lambda_\alpha = 0.005$  throughout this study.

**Evaluation of higher-order statistics for  $\alpha$  output** The predictive probabilities of the statistics  $\phi^D$  and  $\phi^{D_k}$  are evaluated in closed form as follows:

$$\hat{\phi}^D = 1 - \sum_k \int z_k^2 \text{Dir}(z|\alpha) dz = \frac{\alpha_0}{\alpha_0 + 1} (1 - \sum_k \mathbb{E}[z_k]^2), \quad (49)$$

$$\hat{\phi}^{D_k} = 2 \int z_k(1 - z_k) \text{Dir}(z|\alpha) dz = \frac{2\alpha_0}{\alpha_0 + 1} \mathbb{E}[z_k](1 - \mathbb{E}[z_k]). \quad (50)$$

Although an output  $\alpha$  already represents a CPE distribution without ensemble methods such as MCDO and TTA, it can also formally be combined with those methods. In such cases, we can calculate the predictive probability  $\hat{\varphi}$  as follows:

$$\hat{\varphi} = \mathbb{E}_{\hat{q}^{(\text{MC})}(\alpha)}[P(\phi|\alpha)] = \frac{1}{S} \sum_{s=1}^S \mathbb{E}_{z \sim \text{Dir}(\alpha^{(s)})}[P(\phi|z)]. \quad (51)$$

where  $S$  denotes the number of Monte-Carlo samples. The summand in r.h.s can be evaluated in closed form.

## E Experiments with synthetic uncertainty

We conduct an experiment to compare different prediction schemes for CPE distribution of neural networks. As a synthetic dataset, we generate multiple labels for each image instance according to three different uncertainty modes, *i.e.*, high confidence, epistemic uncertainty dominant, and aleatoric uncertainty dominant. Then test whether the predictive CPE distribution of the neural networks can distinguish these modes with an input image of test examples.

### E.1 Experiment setup

**Dataset and preprocessing** We generate a synthetic binary classification problem with the MNIST dataset [20]. As shown in the "Ground truth" row of Fig. 3a, each numeral has a specific distribution of an annotation probability  $q \in [0, 1] \sim P(q)$ , where multiple labels for image  $i$  is drawn from a Bernoulli distribution  $\text{Bern}(q_i)$  in an i.i.d. manner. In this setting, three groups of numerals: 0-1, 2-5, and 6-9 are assigned to different modes of uncertainty: high confidence, epistemic uncertainty dominant (annotators select either label coherently with high probability for each instance, but machines cannot distinguish the difference of the instances), and aleatoric uncertainty dominant (annotators act in uncertain), respectively. Specifically, the instance-wise Bernoulli probability  $q_i$  is generated from either of the following distributions:

$$q_i \sim \begin{cases} \text{Beta}(0.99t\lambda, 0.99(1-t_i)\lambda), & (t_i \in \{0, 1\}) \\ \text{Beta}(0.2(t_i-1)\lambda^{-1}, (1-0.2(t_i-1))\lambda^{-1}), & (t_i \in \{2, 3, 4, 5\}) \\ \text{Beta}(0.2(t_i-5)\lambda, (1-0.2(t_i-5))\lambda), & (t_i \in \{6, 7, 8, 9\}) \end{cases} \quad (52)$$

where  $\lambda = 20$ , and  $t_i$  denotes an original MNIST numeral of the instance  $i$ . We note that the conventional notion of epistemic uncertainty is the one that can be reduced with more data [6]. In other words, the ground truth label is less uncertain, *i.e.*, having higher concordance, than the current model's prediction under the existence of epistemic uncertainty. Although our experimental setup does not directly simulate the former notion of the epistemic uncertainty, we can still test whether the latter one, which is also a unique feature of epistemic uncertainty, is quantified through the inference of CPE distributions.

We examine two scenarios in this experiment. For a common setting, we partition MNIST data into 50,000, 10,000, and 10,000 of training, validation, and test instances, respectively, where one and ten labels per instance are generated in an i.i.d. manner for training and test sets, respectively. The only difference between the two scenarios is the number of labels per instance for the validation set, which are two and five, respectively.

**Deep neural network architecture** We use a neural network architecture with three convolutional and two full connection layers. Specifically, the network has the following stack:

- Conv. layer with 32 channels,  $5 \times 5$  kernel, and ReLU activation
- Max pooling with with  $2 \times 2$  kernel and same padding
- Conv. layer with 64 channels,  $7 \times 7$  kernel, and ReLU activation
- Max pooling with with  $4 \times 4$  kernel and same padding
- Conv. layer with 128 channels,  $11 \times 11$  kernel, and ReLU activation
- Global average pooling with 128 dim. output
- Dropout with 50% rate
- Full connection layer with  $K = 3$  dim. output and softmax activation

**Training** We use the following loss function for training:

$$\mathcal{L}(y, z) = -\frac{1}{\sum_{i=1}^N n_i} \sum_{i=1}^N \sum_{k=1}^K y_{ik} \log z_{ik}, \quad (53)$$

which is equivalent to a negative log-likelihood for instance-wise multinomial distributions except for constant term. While the above loss function returns to an ordinary crossentropy loss for a single-labeled case, the validation loss with multiple labels requires the presented form. We train for a maximum of 100 epochs with a minibatch size of 128, applying early stopping with ten epochs patience for the validation loss improvement.

**$\alpha$ -calibration and predictions** In this experiment, we compare three predictors: CPEs from a raw neural network output, CPE ensembles with MCDO with 20 MC-samples for each instance, and CPE distributions from  $\alpha$ -calibration. We do not include TTA since no image augmentations are applied for the MNIST images. For  $\alpha$ -calibration, we optimize  $\alpha_0$  with the same scheduling and minibatch scheme as the training, except for the loss function, which is described in D.2. For a feature layer used as an input of  $\alpha$ -calibration, we compare the last dropout (last\_do) layer and the last convolutional layer (last\_conv).

## E.2 Results

We examine whether the ground truth distribution of positive class probability  $q$  is predicted as a CPE distribution with each predictive method. For the raw predictor, the mean of CPEs for each numeral (red dashed line in Fig. 3) well matches that of the ground truth. However, the epistemic dominant (numerals of 2-5) and the aleatoric dominant (numerals of 6-9) groups are indistinguishable. This tendency is also retained for MCDO. In contrast, the  $\alpha$ -calibration grasps a difference between the two groups with its CPE distribution, as seen in Fig. 3. In the figure, we compare two feature layers used for  $\alpha$ -calibration, namely, the last dropout layer (last\_do) and the last convolutional layer (last\_conv). Interestingly, the marginal density of the CPE distribution learned with last\_conv for each numeral is much closer to the corresponding ground truth marginal  $q$  distribution than that with last\_do. This fact may suggest that features required to distinguish the two groups disappear near the last classification layer since the expected class frequency for each of the corresponding pairs of numerals between the two groups, i.e., (2, 5), (3, 6), (4, 8), and (5, 9), takes the same value. Among the aleatoric dominant group, the CPE distributions in the scenario with five-fold validation labels are more concentrated and closer to the ground truth than those in the two-fold data.

## F Details of MDS experiments

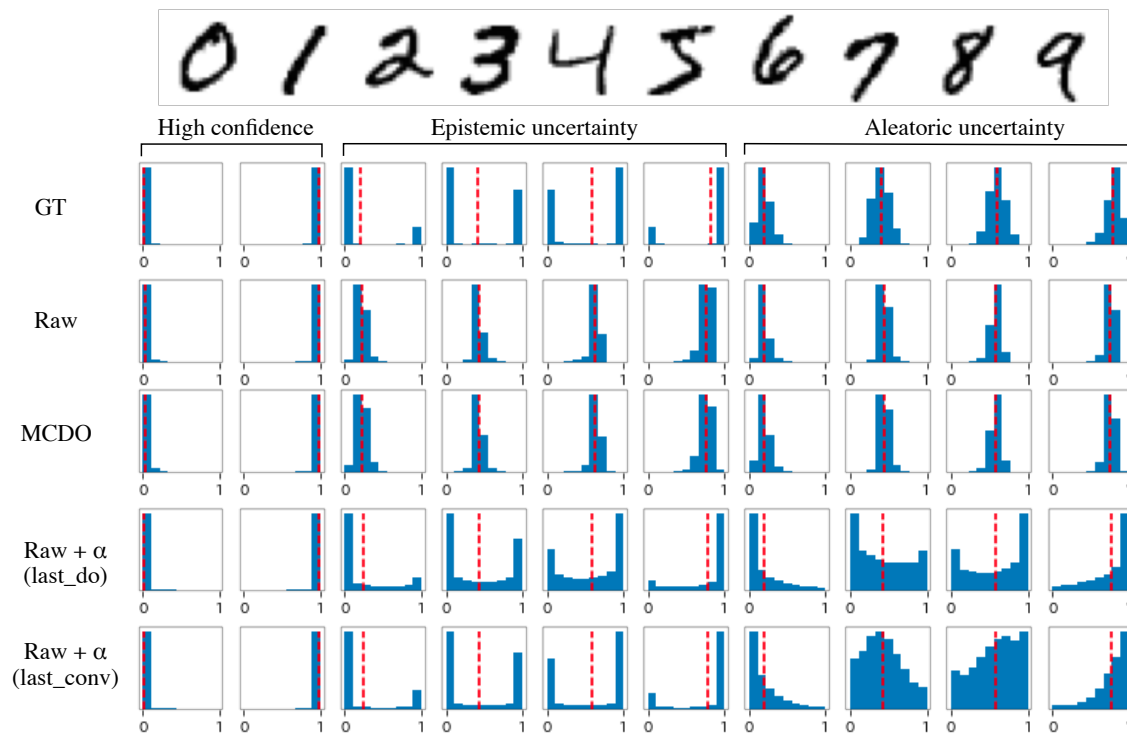
### F.1 Experiment setup

**Dataset and preprocessing** We use 80,610 blood cell images with a size of  $360 \times 363$ , which is a part of the dataset obtained in a study of myelodysplastic syndrome (MDS) [28], where most of the images show a white blood cell in the center of the image. For each image, multiple randomly assigned medical technologists independently annotate a subtype from 22 categories, in which six are anomalous types. We partition the dataset into training, validation, and test set with 55,356, 14,144, and 11,110 images, respectively, where each of the partition consists of images from distinct patient groups. Considering a high labeling cost with experts in the medical domain, we focus on an experimental scenario, where all of the training instances are singly labeled, and multiple annotations are only available for validation and test set. The mean number of labels per instance for validation and test set are 5.79 and 7.58, respectively.

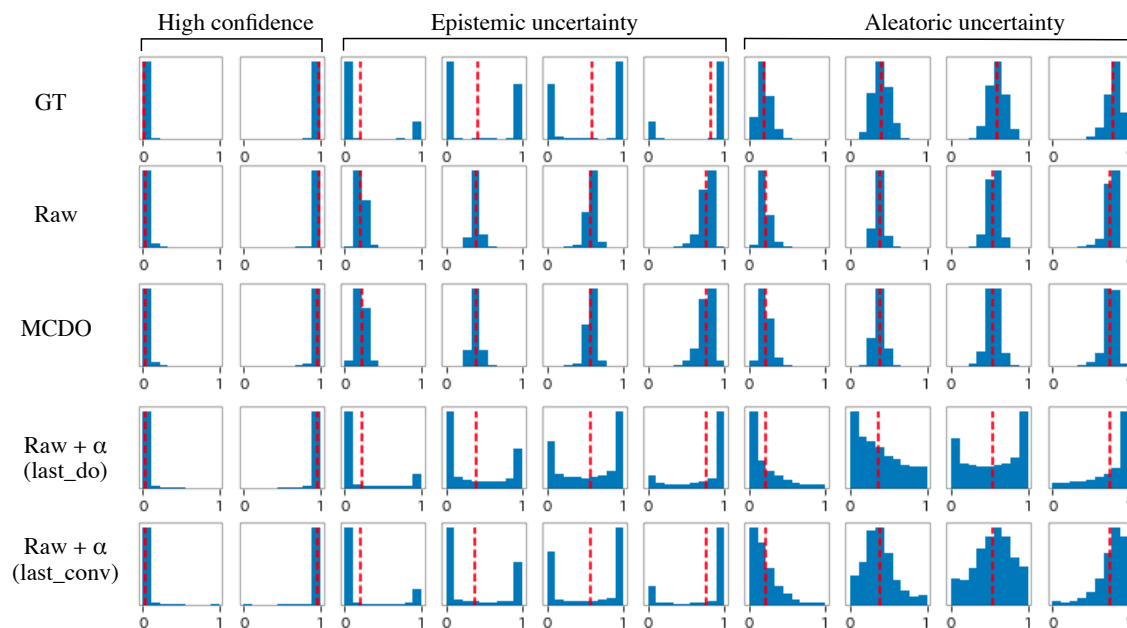
**Deep neural network architecture** We use a modified VGG16 architecture [31] as a base model, in which the full connection layers are removed, and the last layer is a max-pooling with 512 output dimensions. On top of the base model, we append the following layers:

- Dropout with 50% rate and 512 dim. output
- Full connection layer with 128 dim. output and ReLU activation
- Dropout with 50% rate and 128 dim. output
- Full connection layer with 22 dim. output and softmax activation

We use the Keras Framework with Tensorflow backend [4] for implementation.



(a) Marginal density plots for the scenario with two-fold validation labels



(b) Marginal density plots for the scenario with five-fold validation labels

Figure 3: Marginal density plots for the scenario with (a) two-fold and (b) five-fold annotations in the validation set. Ground truth (GT) rows show the distribution of positive class probability  $P(q)$  for each numeral, which is grouped into three modes: high confidence, epistemic uncertainty dominant, and aleatoric uncertainty dominant. A histogram in each row other than GT shows the marginal CPE distribution aggregated for instances within the same numerals. Among the four predictive methods and the two scenarios, the marginal distributions with the last\_conv feature layers and the five-fold validation labels is the closest one to the ground truth distributions.

**Training** We use the loss function shown in equation (53) and Adam [16] optimizer with a base learning rate 0.001, where we use a variant of warm-up and multi-step decay [11] as follows:

- A warm-up with five epochs
- A multi-step decay that multiplies the learning rate by 0.1 at the end of 50, 100, and 150 epochs.

We train for a maximum of 200 epochs with a minibatch size of 128, and record training weights for every five epochs. Then, select the best weights in terms of validation loss. During the training, an input image is processed with a data augmentation followed by cropping the center  $224 \times 224$  portions of the image. The data augmentation applies as a random combination of the following transformations:

- Rotation within  $-180$  to  $180$  degrees
- Width shift within  $\pm 10$  pixels
- Height shift within  $\pm 10$  pixels
- Horizontal flip

We use servers with Intel Xeon CPU E5-2690 v4 and NVIDIA Tesla V100 in our experiments.

**Post-hoc calibrations and predictions** We apply three variants of CPE calibration methods that make a linear transformation to a logit vector before the last softmax activation [10], *i.e.*, temperature scaling (ts), vector scaling (vs), and matrix scaling (ms), in which validation set is used for optimizing weights of the transformation. We use an L2 regularization of intercept for vs, and off-diagonal and intercept regularization [18] (ODIR) for ms. We examine the following hyper-parameter candidates:

- vs:  $\lambda_b \in \{0.1, 1.0, 10\}$
- ms:  $(\lambda_b, \lambda_w) \in \{0.1, 1.0, 10\} \times \{0.1, 1.0, 10\}$

where  $\lambda_b$  and  $\lambda_w$  are defined in equation (47) and (48), respectively. In the CPE calibration, only the weights that transform a logit vector  $u'$  are optimized as described in D.1, where the loss function of equation (53) is used. The validation set is split into 80% calibration and 20% calibration-validation (cv) set. We train for a maximum of 50 epochs using Adam with a learning rate of 0.001, applying early stopping with ten epochs patience for the cv loss improvement. The hyper-parameters are selected with the best cv loss for vs and ms and those are  $\lambda_b = 0.1$  and  $\lambda_b = 1.0, \lambda_w = 10$ , respectively.

The  $\alpha$ -calibration is applied after both the raw training and the CPE calibration. For the feature layer that uses for  $\alpha$ -calibration, we choose a penultimate layer, that corresponds to the last dropout layer in this experiment. The training scheme is the same as that of the CPE calibration, except for a loss function that we described in D.2.

In addition to regular CPEs, which we referred to *Raw* prediction, we also compare options to apply MC-dropout (MCDO) and test-time augmentation (TTA) at prediction time with 20 MC-samples for each of them. A data augmentation applied in TTA is the same as that used in training.